

# Inelastic neutron scattering study of spin gap formation in heavy fermion compounds

D.T. ADROJA<sup>a\*</sup>, K.A. MCEWEN<sup>b</sup>, J.-G. PARK<sup>c</sup>, A.D. HILLIER<sup>a</sup>, N. TAKEDA<sup>d</sup>, P.S. RISEBOROUGH<sup>e</sup>, T. TAKABATAKE<sup>f</sup>

<sup>a</sup>ISIS Facility, Rutherford Appleton Laboratory, Chilton, Didcot, Oxfordshire, OX11 0QX, UK

<sup>b</sup>Department of Physics and Astronomy, and London Centre for Nanotechnology, University College London, Gower Street, London WC1E 6BT, UK

<sup>c</sup>Department of Physics, SungKyunKwan University, Suwon 440-746, Korea and Center for Strongly Correlated Materials Research, Seoul National University, Seoul 151-747, Korea

<sup>d</sup>Faculty of Engineering, Niigata University, Niigata, 950-2181, Japan

<sup>e</sup>Department of Physics, Temple University, Barton Hall, 1900N. 13th Street, Philadelphia, PA 19122, USA

<sup>f</sup>Department of Quantum Matter, ADSM, Hiroshima University, Kagamiyama 1-3-1, Higashi Hiroshima 739-8530, Japan

According to conventional theories of strongly correlated electron systems, the natural consequence of strong hybridization between *f*-electrons and conduction electrons is the opening of a gap in both charge and spin channels. Despite their importance, there are few experimental observations of such gaps in real materials. Recently the charge gap in *d*- and *f*-electron systems has been investigated using optical studies. However, due to the  $q=0$  limitation of the technique, optical studies cannot give information on the wave vector dependence of the gap. Inelastic neutron scattering is a unique technique and provides direct information on the spin gap energy as well as its wave vector and temperature dependence. Further, knowledge of the wave vector dependence of the gap, in particular the spin gap, provides important information about the microscopic mechanism of the gap formation. Recently we have investigated the spin gap formation, and its relation to the charge gap, in several Ce, Yb and U based compounds using inelastic neutron scattering techniques. We review here the nature of the spin gap in CeT<sub>4</sub>Sb<sub>12</sub> (T = Ru, Os and Fe), CeRhAs and U<sub>2-x</sub>Th<sub>x</sub>Ru<sub>2</sub>Sn compounds based on our recent neutron scattering studies. We compare the magnitude of the spin gaps we have measured in this way with that of the charge gaps measured in optical studies. We have found a universal scaling relation between the spin gap energy and the Kondo temperature ( $T_K$ ) for many strongly correlated electron systems and the results are discussed.

(Received

**Keywords:** Spin gap formation, Inelastic neutron scattering investigations, Mixed-valence behaviour, Rare earth and actinide based intermetallic compounds

## 1. Introduction

The strongly correlated electron systems of transition metals and rare-earths/actinides have attracted considerable interest recently due to the duality between the itinerant and the localized nature of *d*- and *f*-electrons that gives rise to a rich variety of novel phenomena, such as mixed valence behaviour, heavy electron behaviour, unconventional superconductivity, Kondo insulator or Kondo semiconductors, spin and charge gap formation, spin and charge density waves, metal-insulator transition and very recently discovered non-Fermi-liquid (NFL) behaviour and quantum criticality [1-5]. These novel properties arise due to the presence of strong electron-electron correlations as revealed by large enhancement of low temperature properties such as the electronic heat capacity coefficient and static susceptibility above the values expected from local density approximation (LDA) electronic-structure calculations [6]. The dual nature and strong electronic correlations are the result of strong hybridization between conduction electrons having spatially extended wave functions and *d*- or *f*-electrons

having localized orbitals. It is still unclear how conduction and localized electrons are reconciled with each other when the local moments are arranged regularly in lattice form (Kondo Lattice). Despite the availability of a large volume of experimental results and many theoretical approaches, a full understanding of the effect of these electron-electron correlations on the physical properties of strongly correlated electron systems is far from complete. Further, it is not clear how the hybridization develops and what is the specific role of transition metals and metalloids in rare-earth and actinide intermetallic compounds.

Among the novel properties mentioned above, the Kondo insulator behaviour observed in *d*- and *f*-electron systems is fascinating and has recently attracted considerable interest in theoretical and experimental condensed matter physics [3-4, 7-17]. These materials exhibit a very small gap, called a hybridization gap, near the Fermi level and it is believed that the gap arises in the lattice, from the hybridization between the localized electrons (*d*- or *f*-electrons) and the conduction electrons [3-4, 9-11]. The main theoretical interest in these materials is due to the existence of large many-body renormalizations. The gaps inferred from optical,

magnetic, transport and thermodynamics properties are almost an order of magnitude smaller than those obtained by band structure calculations [6, 18, 19]. The Kondo insulators usually have cubic symmetry and a mixed-valence character for the  $f$ -elements. The available experimental data suggest that a system with one conduction electron and one spin per unit cell must be an insulator in agreement with the model proposed by Aeppli and Fisk [7]. At high temperatures, the bulk properties of Kondo insulators are similar to those of local moment metals, but at low temperatures, below the characteristic coherence temperature ( $T^*$ ), the conductivity and magnetic susceptibility drop to almost zero. For example, the classical  $d$ -electron system FeSi exhibits a clear signature of an energy gap formation in the optical spectra ( $\Delta_{\text{char}}=50\text{-}90\text{ meV}$ ), in the resistivity ( $\Delta_{\text{tran}}=50\text{ meV}$ ), in the magnetic susceptibility ( $\Delta_{\text{spin}}=64\text{ meV}$ ), that is in fair agreement with *ab initio* band structure calculations ( $\Delta_{\text{char}}=100\text{ meV}$ ) [4, 19]. The detailed discussions on the subject can be found in the review papers by Riseborough [3], Aeppli and Fisk [7], Coleman [4], Degiorgi [8], Tsunetsugu *et al.* [20] and Tselik *et al.* [21].

There are many examples of Kondo insulators in rare-earth and actinide based compounds *exhibiting an energy gap at  $E_F$  with an insulating or semimetallic resistivity and paramagnetic ground state* at low temperatures. For example  $\text{SmB}_6$ , [13]  $\text{YbB}_{12}$  [14],  $\text{Ce}_3\text{Bi}_4\text{Pt}_3$  [15],  $\text{Ce}_3\text{Sb}_4\text{Pt}_3$ ,  $\text{Ce}_3\text{Sb}_4\text{Au}_3$  [22],  $\text{CeFe}_4\text{P}_{12}$  [23],  $\text{CeOs}_4\text{Sb}_{12}$  [24],  $\text{CeRu}_4\text{P}_{12}$  [25],  $\text{CeRu}_4\text{As}_{12}$  [26],  $\text{CeNiSn}$  [16],  $\text{CeRhSb}$  [17],  $\text{CeRhAs}$  [27],  $\text{U}_3\text{Sb}_4\text{Pt}_3$  [28],  $\text{U}_2\text{Ru}_2\text{Sn}$  [29]. In a few Kondo insulator systems *the magnetic ground state co-exists with the Kondo insulating ground state* as in  $\text{UFe}_4\text{P}_{12}$  [23, 30],  $\text{TmTe}$  [31],  $\text{TmSe}$  [32] and  $\text{UNiSn}$  [33]. It is interesting to note that both non-magnetic  $\text{ThFe}_4\text{P}_{12}$  and  $\text{LaFe}_4\text{P}_{12}$  exhibit metallic conductivity down to 4 K [30], which indicates that hybridization is responsible for the gap formation in  $\text{UFe}_4\text{P}_{12}$  and  $\text{CeFe}_4\text{P}_{12}$ . Further it is interesting that  $\text{SmB}_6$  and  $\text{YbB}_{12}$  show in-gap magnetic excitations that exhibit a strong dispersion and temperature dependence [13, 14]. For  $\text{YbB}_{12}$  it has been proposed that antiferromagnetic correlations play an important role in the gap formation [14].

Another interesting behaviour exhibited by many compounds in this class is that they exhibit *an energy gap near  $E_F$ , but with metallic conductivity down to lowest temperatures*. The metallic nature with a small energy gap can be explained when the position of  $E_F$  is outside the gap, i.e. just at the top of the lower hybridized band. Examples of materials in this class are  $\text{CeRu}_4\text{Sb}_{12}$  [34],  $\text{CeFe}_4\text{Sb}_{12}$  [35],  $\text{YbFe}_4\text{Sb}_{12}$  [34] and  $\text{U}_2\text{RuGa}_8$  [36].

Most of the Ce-compounds with an energy gap, mentioned above, exhibit a broad maximum in their susceptibility, indicating the mixed valence nature of the Ce ion. We mention here for the sake of completeness that there are a few interesting Ce-based compounds that exhibit an energy gap in transport or NMR/tunnelling, but whose susceptibility behaviour reveals the Ce ion to be in a trivalent state. For example,  $\text{CeRu}_4\text{Sn}_6$  reveals an interesting interplay of strong correlations and an NFL-like state at low temperatures, and gap formation and a carrier-deprived state that develops at intermediate temperatures [37]. The first indication of the possible

formation of an energy gap in  $\text{CeRu}_4\text{Sn}_6$  comes from the electrical resistivity measurements [37], which have recently been confirmed through NMR measurements yielding the gap of  $\Delta/k_B \approx 124\text{ K}$  [38]. The specific heat  $C(T)/T$  of  $\text{CeRu}_4\text{Sn}_6$  is large and logarithmically divergent below  $\sim 2\text{ K}$ , in spite of the fact that its electronic contribution ( $\gamma T$ ) between 8 and 10 K is *less* than that of the normal-metal non- $f$ -electron counterpart  $\text{LaRu}_4\text{Sn}_6$ . This is a strong indication of a low carrier-density state in  $\text{CeRu}_4\text{Sn}_6$ . Another example in this class is  $\text{CeCuAs}_2$ , which exhibits Curie-Weiss behaviour in the susceptibility above 100 K, but has a negative temperature coefficient of electrical resistivity down to 45 mK, *i.e.* a very similar behaviour to that of Kondo insulators [39]. Preliminary tunnelling spectroscopy measurements indicate the existence of a pseudogap at least at low temperatures, implying that this compound could be classified as a Kondo semiconductor [40], though its thermoelectric power is found to be different from that of an activated type Kondo insulator. Further,  $\text{CeRhSn}$  exhibits a strong anisotropy in the susceptibility and resistivity, together with NFL behaviour in the susceptibility, resistivity and heat capacity [41]. However, our low energy and high energy inelastic neutron scattering study clearly reveals a gap type excitation centred near 25-30 meV, without any clear presence of quasi-elastic scattering [42].

It has been reported that NMR measurements on the quasi-one dimensional compounds  $\text{RMn}_4\text{Al}_8$  ( $R=\text{La, Ce, Y}$  and  $\text{Lu}$ ) also show clear evidence of a spin gap formation near  $E_F$  [43]. The spin gap nature of the gap in  $R=\text{Y}$  and  $\text{La}$  compounds has been confirmed through recent inelastic neutron scattering measurements [44]. Interestingly,  $\text{YMn}_4\text{Al}_8$  reveals a clear sign of a 27 meV spin gap for a limited range of wave vectors, which may suggest that the mechanism of the gap formation in these compounds is different from that attributed to Kondo insulator systems [3-4, 7-17]. It is to be noted that the difference between FeSi and  $f$ -electron Kondo insulators becomes apparent when doped: whilst the former exhibits enhanced susceptibility leading to a Stoner-like ferromagnetic instability, the latter are usually characterized by competition between the Kondo screening and local moment magnetism with RKKY inter-site coupling.

Although the physics of high temperature superconductors (HTSC) is different from Kondo insulators, we note that the pseudogap phenomena have recently attracted much attention with pseudogap features, of both spin and charge gaps, observed in HTSC, especially in the underdoped regime [45, 46]. Therefore the pseudogap phenomenon in HTSC has attracted considerable interest due to its possible connection to the mechanism of high  $T_C$  superconductivity. Many experiments observed that the density of states at  $E_F$  reduces gradually below a pseudogap onset temperature [45]. Even though it is not applicable to the wide range of HTSC compounds, there has been an attempt to correlate the spin gap value with the superconducting transition temperature ( $T_C$ ) for electron doped HTSC materials [46].

Recently the optical study of many heavy fermion systems by Okamura *et al.* [47] reveals a universal scaling relation between the mid-IR peak energy (which we call a charge gap) and the Kondo temperature,  $E_{\text{MIR}} \sim (T_K W)^{1/2}$ ,

where  $W$  is the width of bare conduction band. It should be emphasised that although the optical studies are successful in finding the charge gap in heavy fermion systems they cannot offer any further information about the  $Q$ -dependence of the gap, due to the limitations of this technique: any indirect optical transitions (i.e.  $\partial Q \neq 0$ ) are forbidden by the momentum conservation rule within first order optical processes [48]. However, one should note that non-dipolar transitions with  $\partial Q \neq 0$  are possible in the second order optical process through which a two-phonon process occurs [49]. Thus it would be very interesting to investigate if there exists any relation between the spin gap and  $T_K$ . In order to answer this question we have recently carried out inelastic neutron scattering investigations in many heavy fermion systems and our detailed results are published in refs. [50-55]. In the present work we review the spin gap formation in  $\text{CeT}_4\text{Sb}_{12}$  ( $T=\text{Ru, Os, Fe}$ ),  $\text{CeRhAs}$  and  $\text{U}_{2-x}\text{Th}_x\text{Ru}_2\text{Sn}$  using the inelastic neutron scattering technique. Our studies clearly reveal that, like the optical scaling behaviour, there exists a universal scaling relation between the single ion Kondo temperature and the spin gap energy in heavy fermion systems. Further, our studies indicate that single ion type interactions are important for the spin gap in  $\text{CeT}_4\text{Sb}_{12}$  ( $T=\text{Ru, Fe and Os}$ ), while the Kondo lattice of the  $U$ -atoms plays an important role in the spin gap formation in  $\text{U}_2\text{Ru}_2\text{Sn}$ .

## 2. Theoretical discussion

The physics of heavy fermion systems at high temperatures is dominated by single impurity Kondo scattering and can be well understood within the Anderson impurity model (AIM), where the localised  $d/f$  orbital with spin  $S$  and a degeneracy  $N_f = 2S + 1$  is hybridized with the conduction band electrons [56]. The AIM is one of the most important models for the understanding of strong correlations in condensed matter physics. It is relatively simple and captures the most essential feature of strong correlations, namely the large Coulomb repulsion ( $U$ ) between electrons that exceeds their kinetic energy: the details of the interaction terms in the Hamiltonian can be found in refs. [3, 56]. In this model a sharp fermionic resonance peak develops near  $E_F$ , whose magnitude increases with decreasing temperatures (Fig.1a). The high density of electrons, having mainly  $4f$  character, in the resonance peak, gives rise to an enhanced value of the heat capacity and magnetic susceptibility at low temperatures and a  $-\ln(T)$  dependent resistivity at high temperatures. Furthermore, the width of the peak provides an estimate of the Kondo temperature,  $T_K$ . Nozières (1974) [57] and Nozières and Blandin (1980) [58] considered the spin-fluctuation limit of this model, and demonstrated that its low-temperature properties can be described in terms of a local Fermi liquid theory.

The AIM, however, fails in explaining some of the observed properties of a dense Kondo system (Kondo lattice), where Kondo centres are arranged in a form of lattice (Fig.1b), and exhibits an onset of coherence below a characteristic temperature,  $T^*$ . Below  $T^*$ , strong elastic scattering disappears and individual Kondo centres coherently scatter conduction electrons. The simplest

theoretical model to describe the behaviour of dense Kondo lattices and Kondo insulators is the periodic Anderson model (PAM) [3]. This model is exactly solvable in the non-interacting limit when  $U \rightarrow \infty$ . Riseborough [3] has obtained the solution for the PAM with orbital degeneracy  $N = 2$ , in the mean-field slave-boson approximation. At half filling this exhibits a direct gap (which we denote as the charge gap,  $\Delta_{\text{char}}$ ) at  $q = 0$  and an indirect gap (spin gap,  $\Delta_{\text{spin}}$ ) at  $q \neq 0$  in the fermionic density of states near  $E_F$  (Fig.1b). The magnitude of the indirect and direct gaps are given by  $2V^2/W$  and  $2V$ , respectively, where  $W$  is the half width of the conduction band and  $V$  is the hybridization matrix element. The electronic state of the renormalized bands has a mixed character of  $f$  electron and conduction band electrons. Further, the  $f$ -DOS of the upper hybridized band has a maximum near the zone centre, while that of the lower hybridized band has a maximum near the zone boundary (Fig.1c). We recall that the neutron scattering cross-section, given by Fermi's Golden rule, is proportional to the square of the matrix elements of the DOS of the initial and final states. It is to be noted that for the case when  $E_F$  (or the chemical potential) lies in the middle of the gap the system exhibits insulating-type resistivity. On the other hand, when  $E_F$  lies at the top of the lower hybridized band, the system exhibits metallic-type resistivity in spite of the presence of the energy gap.

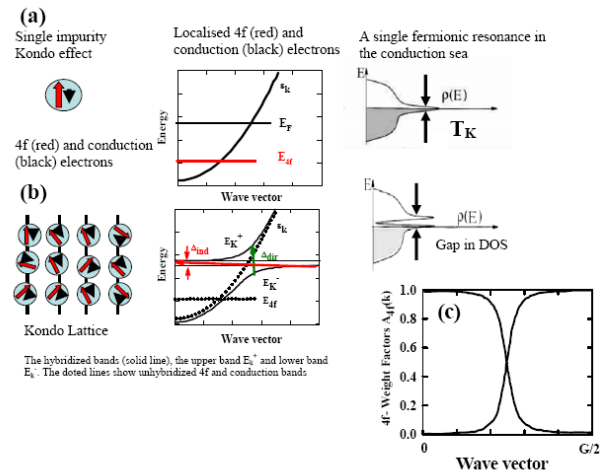


Fig. 1 (color online) (a) Single impurity Kondo effect, a schematic view of the conduction electron band and localised  $4f$ -electron, and resonant density of states (DOS) showing build up of the fermionic resonance near the Fermi level. (b) Kondo lattice case, hybridized band picture showing renormalized bands, lower ( $E_K^-$ ) and upper ( $E_K^+$ ) hybridized bands, and direct gap,  $\Delta_{\text{dir}}$  (we called charged gap,  $\Delta_{\text{char}}$ ) at  $q = 0$  and indirect gap,  $\Delta_{\text{ind}}$  (we called spin gap,  $\Delta_{\text{spin}}$ ) at  $q \neq 0$  and the gap in resonant density of states (DOS). (c) The  $4f$ -weight factors of the upper and lower bands as a function of wave vector, taken from Riseborough [3, 4].

As a further development on theoretical explanations of Kondo insulators, Ikeda and Miyake have obtained the

solution of the PAM, to understand the Kondo insulator behaviour of CeNiSn, by introducing anisotropic hybridization  $V(\mathbf{k})$ , which vanishes precisely along one direction, i.e. along the  $z$ -axis [59]. On the other hand, the Moreno and Coleman theory for CeNiSn found that there exist three global minima and three local minima in the CEF parameter space with small differences in their free energies among the favourable states [10]. Jarrell *et al.* have also studied the symmetric periodic Anderson model in the limit of infinite dimensions within the quantum Monte Carlo method [9]. They have shown that a gap forms in the single particle spectral function as well as in the neutron structure factor. Further, their study shows that, depending on the relative strength of the gap energy and other energy scales in the system, there is a transition from a paramagnetic state to an antiferromagnetic state.

Recently a theoretical model was proposed for the pseudo-gap formation in Ce, Sm, Eu and Yb based compounds by Hanzawa [11], who discussed the various limits of CEF and its roles in the gap formation. Their model considered a variety of energy gap features depending on the strength and symmetry of the CEF. The three cases they discussed are: (i) No CEF effect - in this case a fully isotropic gap opens at the Fermi level, (ii) Large CEF effect - if the CEF splitting is large enough, then an anisotropic full or pseudo-gap opens, and (iii) Intermediate CEF effect - when  $\Delta_{\text{CEF}} \sim \Delta_{\text{gap}}$ , then rather complicated but interesting features appear in the gap formation [11]. As shown for the  $J=5/2$   $\text{Sm}^{3+}$  case with a cubic crystal field, a full gap opens for the case of the  $\Gamma_8$  ground state, while a small but finite density of states remains in the pseudo-gap region for the  $\Gamma_7$  ground state. Although Hanzawa *et al.* did not discuss the case of  $\text{Ce}^{3+}$ , it is not unrealistic that as  $\text{Ce}^{3+}$  also has  $J=5/2$  one can apply a similar theoretical approach to explain the gap formation in Ce-based Kondo insulators.

A different theoretical approach based on spin fluctuations has been considered by Liu [60] to explain the gap formation in  $\text{YbB}_{12}$ . In his model, the gap in the  $f$ -electron system originates from local effects and tends to persist in incoherent systems. In a coherent periodic lattice the gap has dispersion, in qualitative agreement with single crystal neutron scattering experiments [14]. In essence, the theory by Liu follows the same line as the spin-fluctuation theory for metals except for differences in mathematical details necessitated by the insulating state. The phenomenological model derived with a reasonable approximation explains the bulk properties and their temperature dependence as well as the inelastic neutron scattering line shape for powder samples. Tsvelik [21] has also studied the one dimensional model of the Kondo lattice at half-filling, which shows that the insulating state forms not due to a hybridization of conduction electrons with local moments, but as a result of strong antiferromagnetic fluctuations. This model does not require a global antiferromagnetic ordering and the spin ground state remains disordered with a finite correlation length.

### 3. Aim of the present studies

Despite intensive theoretical as well as experimental studies over the past two decades, a full understanding of the mechanism of gap formation in strongly correlated electron systems is still lacking. In particular, the roles played by the local Kondo coupling and the inter-site correlations in the gap formation and its anisotropic nature are not well understood. For example, the optical and inelastic neutron scattering studies on  $\text{YbAl}_3$  clearly reveal the presence of a hybridization gap [61]. However, the recent theoretical calculations based on PAM by Kuroiwa *et al.* indicate the absence of a hybridization gap [61]. Recent optical conductivity studies show a strongly temperature dependent response in  $\text{CeT}_4\text{Sb}_{12}$  ( $T=\text{Ru, Fe and Os}$ ) systems with clear evidence of charge gap formation in the strongly hybridized band near  $E_F$  [62-64]. The key question regarding the charge gap feature found in  $\text{CeT}_4\text{Sb}_{12}$  is whether it is somehow connected to the spin degrees of freedom so as to produce a corresponding spin gap in the magnetic excitation spectrum, which is then observable by inelastic neutron scattering. If such a spin gap indeed exists, then it is important to determine whether it is  $Q$ -dependent (indicating inter-site coupling) or  $Q$ -independent (*i.e.* a single ion feature). An experimentally determined ratio between the spin gap and charge gap energies is also important from a theoretical point of view. Thus it is important to carry out systematic experimental and theoretical investigations on spin and charge degrees of freedom on strongly correlated  $d$ - and  $f$ -electron systems using various experimental techniques to obtain a complete physical picture of the gap formation. In the present work, we therefore have investigated the spin degrees of freedom in many strongly correlated electron systems using the inelastic neutron scattering technique and our results are discussed here.

#### 3.1 $\text{CeRu}_4\text{Sb}_{12}$ : A single spin gap system

##### 3.1.1 Crystal structure and bulk properties

$\text{CeRu}_4\text{Sb}_{12}$  is a member of the filled skutterudite family with a general formula  $\text{RT}_4\text{X}_{12}$  ( $R$ =rare-earth elements,  $T = \text{Fe, Ru, Os}$  and  $X = \text{Sb and P}$ ) and crystallizes in a unique body-centred-cubic structure, space group  $I m \bar{3}$  (see Fig.2). Interestingly, the cubic structure of skutterudite compounds has the large  $X_{12}$ -icosahedron atomic cages filled with rare-earth atoms. Due to the availability of a large empty space around the rare-earth atoms, their amplitude of thermal vibrations is an order of magnitude larger than that of  $T$  and  $X$  atoms. As a result of the larger thermal motion, the lattice thermal conductivity is remarkably small. This result has led to a speculation that the rattling motion of the rare-earth atoms (so-called Einstein modes) may strongly scatter acoustic phonons, which carry most of the heat flow in a crystal, resulting in an anomalous suppression of the lattice thermal conductivity. Hence filled skutterudite compounds have an enhanced value of the thermoelectric figure of

merit and are considered as potential candidates for future solid-state device technology in related industries.

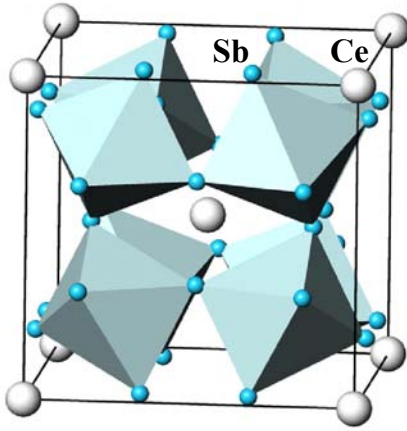


Fig.2 (color online) The cubic unit cell of  $\text{CeRu}_4\text{Sb}_{12}$  compound; Ru atoms are located in the centre of the  $\text{Ru}_4\text{Sb}_{12}$  octahedra.

On the other hand, the bulk properties  $\text{CeRu}_4\text{Sb}_{12}$  are of particular interest due to their strongly correlated electronic behaviour. The intermediate valence behaviour of  $\text{CeRu}_4\text{Sb}_{12}$  has been seen in its magnetic susceptibility and electrical resistivity, see Fig.3a&c [34, 65, 66]. The susceptibility exhibits a maximum around 100 K, which provides an estimate of the Kondo temperature of  $T_K = 300$  K: according to the single-impurity Anderson model,  $T_K = 3T_{max}$ , where  $T_{max}$  is the temperature at which the susceptibility exhibits a broad maximum [67]. Furthermore, the magnetic contribution to the resistivity of  $\text{CeRu}_4\text{Sb}_{12}$ , deduced by subtracting the resistivity of the isostructural nonmagnetic compound  $\text{LaRu}_4\text{Sb}_{12}$ , shows a maximum near 80 K. Above this temperature, the resistivity shows a clear  $-\ln(T)$  dependence, while below 80 K it decreases dramatically due to an onset of coherence [66]. The temperature dependence of the resistivity (Fig. 3c) thus implies that  $\text{CeRu}_4\text{Sb}_{12}$  forms a coherent Kondo lattice state below about 80 K [66].

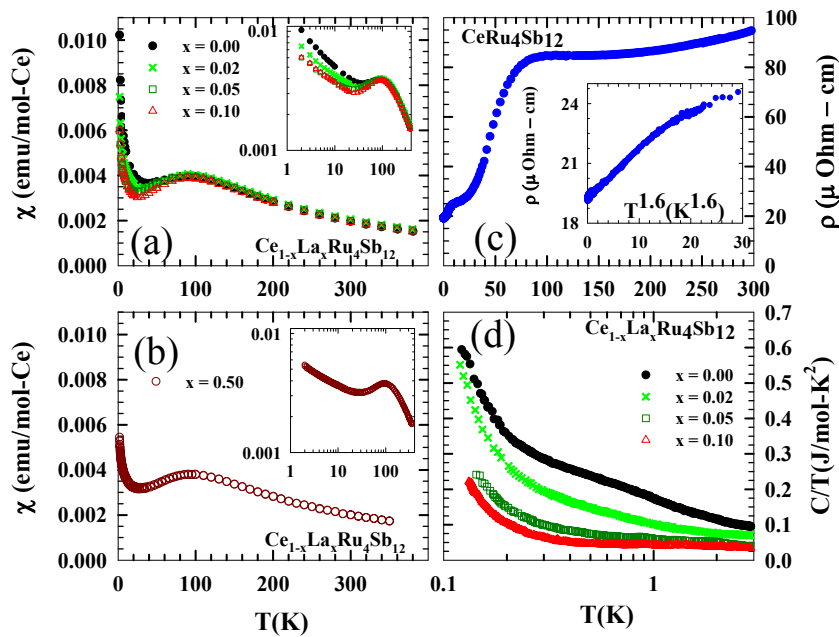


Fig. 3. (a-b) Magnetic susceptibility versus temperature (the inset shows log-log plot) for  $\text{Ce}_{1-x}\text{La}_x\text{Ru}_4\text{Sb}_{12}$  ( $x=0$  to  $0.5$ ), (c) resistivity versus temperature (the inset shows  $\rho(T)$  vs  $T^{1.6}$ ) for  $\text{CeRu}_4\text{Sb}_{12}$ , and (d) the electronic contribution of the heat capacity divided by temperature ( $C_{ele}/T$ ) versus  $\log(T)$  for  $\text{Ce}_{1-x}\text{La}_x\text{Ru}_4\text{Sb}_{12}$  ( $x=0$  to  $0.1$ ), after Takeda et al. [34]; the susceptibility data of  $x = 0.5$  are from the present work.

Interestingly, the electronic contribution to the heat capacity of this compound is rather large  $\gamma = 380$  mJ/mol-K<sup>2</sup> [65]. This large electronic heat capacity undoubtedly suggests that the low-temperature states of this compound are of moderately heavy fermion origin. More interestingly, the low temperature (below 1 K) heat capacity (Fig.3d) and susceptibility exhibit logarithmic behaviour, whilst the resistivity reveals a  $T^n$  behaviour with  $n = 1.6$ , see the inset Fig.3c [65, 68]. These unusual

low temperature properties have been interrelated due to NFL behaviour. It is to be noted that the low temperature (below 20K) susceptibility can also be fitted by power law behaviour as predicted for the NFL behaviour in the Griffiths' phase model [68]. Recently, an upturn of the Hall coefficient and a loss of the low-frequency intensities in the optical conductivity at low temperatures were reported in  $\text{CeRu}_4\text{Sb}_{12}$  [62, 66]. These experimental results suggest a reduction in the carrier density at low

temperatures and the opening of a charge gap  $\Delta_{charge} = 47$  meV as inferred from the optical study [62]. Here the charge gap means a gap in the charge degrees of freedom. Further, the infrared study of  $\text{CeRu}_4\text{Sb}_{12}$  in applied fields up to 17 T reveals that the applied magnetic field strongly affects the low-energy excitations in the system [69]. In particular, the magnitude of the quasi-particle mass has been suppressed by as much as 25% at 17 T at 10 K [69]. This effect is in quantitative agreement with the mean-field solution of the periodic Anderson model augmented with a Zeeman term [69]. Ultrahigh-resolution photoemission spectra of  $\text{CeRu}_4\text{Sb}_{12}$  reveal crossover behaviour into a low carrier state [70]. The DOS around the  $E_F$  decreases on lowering the temperature and a semi-metallic-like DOS is observed at 5.9 K. The temperature dependence of the DOS at  $E_F$  is explained in terms of the development of the coherence. Thus in order to understand the nature of the spin degrees of freedom in  $\text{CeRu}_4\text{Sb}_{12}$ , we have carried out detailed inelastic neutron scattering measurements [50, 51] and the results are summarized below.

### 3.1.2 Inelastic neutron scattering study: A single spin gap system

A detailed inelastic neutron scattering investigation on  $\text{CeRu}_4\text{Sb}_{12}$  as well as on the non-magnetic reference compound  $\text{LaRu}_4\text{Sb}_{12}$  has been reported by Adroja *et al.* [50, 51]. The magnetic response of  $\text{CeRu}_4\text{Sb}_{12}$ , after subtracting the phonon background, is shown for several temperatures in Fig. 4.

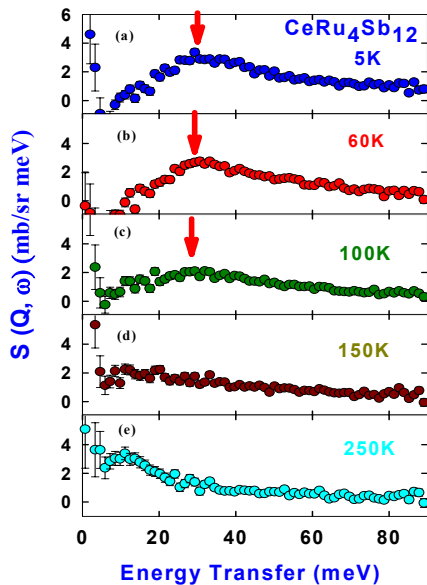


Fig. 4. (color online) (a–e) The magnetic response from  $\text{CeRu}_4\text{Sb}_{12}$  at low scattering angles ( $19^\circ$ ) after subtracting off the nonmagnetic scattering at several temperatures [51]. The arrow shows the position of the spin gap.

As can be seen in Fig. 4a for 5 K, the magnetic scattering is almost absent for energy transfers below 10–15 meV, but exhibits a broad peak at 30 meV. According to theoretical studies [71], the peak position can be

regarded as an estimate of the magnitude of the spin gap. For energy transfers higher than 30 meV, the magnetic scattering falls off gradually and there is still a visible sign of magnetic scattering even at the energy transfer of 95 meV. On increasing the temperature to 60 K, there is very little change in the data regarding the intensity, position, and width of the magnetic scattering, see Fig. 4b. It is to be noted that the first visible temperature dependence was observed when the sample was heated through the coherence temperature of  $T_{coh} = 80$  K. As shown in Fig. 4c, the spin gap feature starts to fill up at 100 K while the peak position hardly moves compared with the data taken at lower temperatures. We recall that the static magnetic susceptibility also exhibits a maximum at 100 K, which implies  $T_K = 300$  K according to the single-impurity Anderson model [67]. It is to be noted that for valence-fluctuating systems the position of an inelastic peak can be taken as an estimate of the Kondo temperature [72]. A further rise in temperature to 150 K completely destroys the gap in the magnetic response, which can now be described by a broad quasielastic peak. At 250 K, some intensity of the magnetic scattering at high energy transfers shifts towards lower energies and its shape becomes purely quasielastic. We note that the peak-like structure seen near 10 meV at 250 K is an artifact arising from the difficulties of making a precise subtraction of the elastic line. The overall drastic change in the magnetic response between 60 and 250 K again suggests that the temperature dependence of the spin gap is quite different from that of a conventional band-structure gap. The collapse of the inelastic gap-like response and the appearance of the quasielastic scattering at higher temperatures observed in  $\text{CeRu}_4\text{Sb}_{12}$  are similar to that observed in  $\text{YbAl}_3$  and  $\text{Ce}_3\text{Bi}_4\text{Pt}_3$  [72, 73] and also in agreement with the predictions of theoretical models [3, 7, 74]. It is to be noted that the spin gap of 60 meV observed (at 5 K) in  $\text{U}_2\text{RuGa}_8$  does not show a dramatic change in the response at 300 K compared with that of 5 K [36]. By performing a numerical integration over the whole experimental energy transfer range up to  $\pm 97$  meV, and using the moment sum rule of  $S(Q, \omega)$ ,  $\int S(q, \omega) / F^2(Q) d\omega = 48.8 \mu_{eff}^2$ , we have deduced the value of the effective magnetic moment to be  $\mu_{eff} = 2.1(\pm 0.3) \mu_B$  at 5 K. An alternative determination of the moment was carried out by extrapolating the data to high energy, up to 290 meV, by fitting the data to an exponential decay function between 30 and 97 meV, which gave an estimate of  $\mu_{eff} = 2.6(\pm 0.4) \mu_B$ , indicating that magnetic response has transferred to high energy at 5 K.

We now discuss the wave vector  $|Q|$  dependence of the magnetic response. In Fig. 5, we show a contour plot of the magnetic scattering at 5 K as function of energy transfer and  $|Q|$ . It is clear from the contour plot that the scattering exhibits a broad peak at 30 meV and its position is independent of  $|Q|$ . The integrated intensity between 30 and 50 meV exhibits behaviour similar to that of the square of the  $\text{Ce}^{3+}$  magnetic form factor. This behaviour further confirms the nearly  $Q$  independent of the magnetic response and hence the  $Q$  independent spin gap

in  $\text{CeRu}_4\text{Sb}_{12}$ , implying that single ion type interactions are playing an important role in the gap formation.

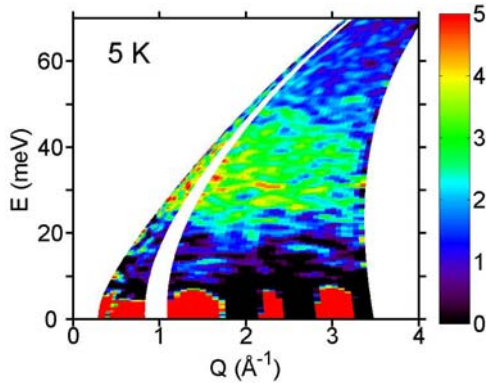


Fig. 5. (color online) The contour map of the magnetic scattering taken at 5 K as function of energy and  $Q$ , taken from ref [51].

### 3.1.3 Low energy excitations

In heavy fermion systems the linewidth of the quasielastic scattering from the ground state crystal field level provides information about  $T_K$ . The main question here is whether there will also be any quasi-elastic scattering presence when we have a hybridization gap open at  $E_F$ . Riseborough has shown theoretically that one can have intra-band excitations with thermally activated integrated intensity, and should have the form of a quasi-elastic spectrum which also exists within the gap region [3]. Further the quasi-elastic scattering may develop from spin fluctuations allowed by *spin holes* created in the lower hybridized band by the replacement of nonmagnetic La for Ce. As pointed out by Riseborough [3], such intra-band scattering is expected to be weak and distributed over a wide range of energies. To find out whether there exists such quasi-elastic scattering in  $\text{CeRu}_4\text{Sb}_{12}$ , we have carried out high resolution and low energy inelastic neutron scattering measurements on the IRIS spectrometer, which has a resolution of 0.08 meV (FWHM) at the elastic energy. Our study did not reveal any clear sign of quasi-elastic scattering at 4 K in  $\text{CeRu}_4\text{Sb}_{12}$ . This may suggest that gap opens over the entire Fermi surface or the quasi-scattering is too weak to be detectable.

#### 3.1.3.1 $\text{Ce}_{1-x}\text{La}_x\text{Ru}_4\text{Sb}_{12}$ ( $x = 0-0.5$ ): Importance of single ion Kondo interactions in the gap formation

The gaps observed in the Kondo insulator are extremely sensitive to doping in which  $f$ -electron atoms are substituted by non- $f$ -electron atoms. The effect of disorder (or impurities) on the spin gap formation has been theoretically investigated using the PAM at half filling by Riseborough [75]. The effect of the impurities is treated within the coherent potential approximation (CPA).

According to this calculation, the substitution of non- $f$ -impurities on the  $f$ -sites produces an impurity band within the gap, and a few percent of impurity concentration leads to an impurity band that spans the entire gap. The main effect of doping is thus to reduce the gap in the wave vector averaged spectral density and to introduce states within the gap, as observed experimentally in the inelastic neutron study of  $(\text{Ce}_{1-x}\text{La}_x)_3\text{Bi}_3\text{Pt}_3$  [73]. It is therefore interesting to investigate the effect of La-doping on the spin gap formation in  $\text{CeRu}_4\text{Sb}_{12}$ .

The bulk properties of  $\text{Ce}_{1-x}\text{La}_x\text{Ru}_4\text{Sb}_{12}$  ( $x=0-0.1$ ) have been reported by Takeda *et al.* [34,65]. Surprisingly the NFL behaviour observed in the heat capacity at low temperatures for  $x = 0$  has been suppressed completely for  $x = 0.1$  (10 % La-doping) (see Fig. 3d). Very similar behaviour has also been observed in the low temperature susceptibility (Fig. 3a). More interestingly, the susceptibility behaviour at high temperature is not affected by La-doping as high as 50 % (Fig. 3b). We have also measured the susceptibility of a  $\text{Ce}_{0.2}\text{La}_{0.8}\text{Ru}_4\text{Sb}_{12}$  single crystal that exhibits a maximum near 90 K and very similar temperature dependence to that observed in  $x = 0-0.5$ , but the magnitude of the susceptibility was found to be negative, which we attribute to the diamagnetism from the Sb-flux. These results reveal that the observed maximum in the susceptibility of  $\text{CeRu}_4\text{Sb}_{12}$  at 100 K is nearly independent of the La-doping. This may suggest that the spin gap still exists in the La-doped samples. Thus in order to confirm the presence of the spin gap in  $\text{Ce}_{1-x}\text{La}_x\text{Ru}_4\text{Sb}_{12}$  ( $x=0-0.5$ ), we have also investigated  $x=0.5$  compound using inelastic neutron scattering measurements. The magnetic response obtained from  $\text{Ce}_{1-x}\text{La}_x\text{Ru}_4\text{Sb}_{12}$  ( $x=0.5$ ) compound, after subtracting the non-magnetic phonon contribution, is plotted in Fig.6b: for comparison we have also plotted the response from  $x=0$  in Fig.6a. It is clear from Fig.6 that the magnetic response of  $x=0.5$  reveals a broad peak near 30 meV as seen in the parent  $\text{CeRu}_4\text{Sb}_{12}$  compound. Considering the observed peak in the susceptibility, which is also related to  $T_K$  and hence with the spin gap energy (discussed below), we interpret the observed inelastic peak in  $x = 0.5$  as due to the presence of the spin gap. It would be interesting to carry out an optical study on  $x=0.1-0.8$  alloys to find out whether the charge gap does exist in these compositions. The susceptibility behaviour together with the inelastic neutron scattering confirm that the spin gap in  $\text{Ce}_{1-x}\text{La}_x\text{Ru}_4\text{Sb}_{12}$  arises due to the single ion type interactions and not Kondo lattice formation as required in the theoretical models [3, 8-11]. Very similar conclusions have been obtained for the observed anomalous properties at low temperature and gap formation in  $\text{Ce}_{1-x}\text{La}_x\text{Os}_4\text{Sb}_{12}$  ( $x=0, 0.02$  and  $0.1$ ) through the heat capacity, resistivity and magnetic susceptibility measurements [76]. In these compounds the transport gap and the maximum in the susceptibility, which is related to  $T_K$  and hence the spin gap, have been found to be independent of the La-doping. However, the low temperature heat capacity and magnetic susceptibility are very sensitive to the La-doping [76] and decrease dramatically with increasing La-concentrations similar to that observed in  $\text{Ce}_{1-x}\text{La}_x\text{Ru}_4\text{Sb}_{12}$ .

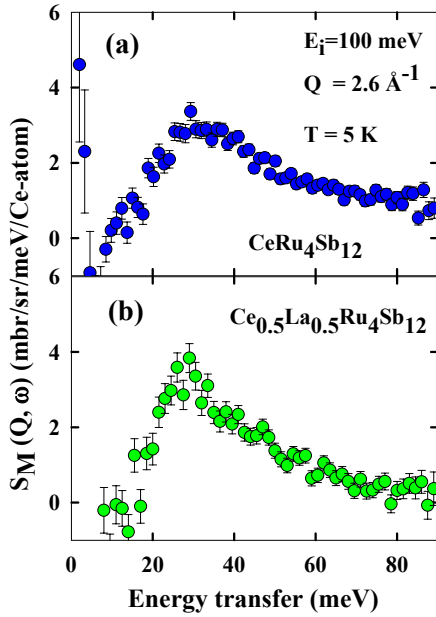


Fig. 6 (color online) (a-d) The magnetic response from  $Ce_{1-x}La_xRu_4Sb_{12}$  ( $x=0$  and  $0.5$ ) at low scattering angles ( $19^\circ$ ) after subtracting off the nonmagnetic scattering at 5 K

It is interesting to compare the results of  $Ce_{1-x}La_xRu_4Sb_{12}$  with those of  $(Ce_{1-x}La_x)_3Bi_4Pt_3$  (0 to 0.25). In the latter system, the La-doping acts to progressively decrease the energy gap with increasing  $x$ , as seen through inelastic neutron scattering measurements [73]. This is also in agreement with the observed decrease in the value of  $T_{max}$ , at which the susceptibility exhibits a maximum and a decrease in the activation energy observed through the resistivity [77]. The decrease of the energy gap with increasing  $x$  tracks similar behaviour in the single ion Kondo temperature [77]. The existence of a spin gap even for  $x = 0.25$  suggests that coherence effects are not as significant as most of the theories have predicted, and that the spin dynamics are more or less governed by local physics. Possibly, the gap suppression with increasing  $x$  is caused by negative chemical pressure created by expanding the lattice with La substitution, which is consistent with the charge gap increasing with applied pressure.

### 3.2 CeOs<sub>4</sub>Sb<sub>12</sub>: Two spin gaps

#### 3.2.1 Crystal structure and bulk properties

CeOs<sub>4</sub>Sb<sub>12</sub> is also a member of the skutterudite family and crystallizes in the cubic structure, which is discussed previously in section 4.1a. The first evidence of Kondo insulating behaviour with a very small transport gap of 10 K in CeOs<sub>4</sub>Sb<sub>12</sub> was reported from the transport measurements [24]. The resistivity is metallic at room temperature, but increases strongly, with decreasing temperatures, below 50 K. On the other hand, the specific

heat coefficient,  $\gamma \sim 90\text{-}180 \text{ mJ mole}^{-1} \text{ K}^{-2}$  [24, 78-79] and enhanced Pauli susceptibility indicate strongly correlated electron behaviour of CeOs<sub>4</sub>Sb<sub>12</sub> [24]. The temperature dependence of the susceptibility exhibits a broad maximum near 100 K, which can be explained using either a crystalline electric field (CEF) model with a CEF splitting of  $\sim 28 \text{ meV}$  for the  $Ce^{3+}$  ion [24] or a valence fluctuation model.

Interestingly, the optical conductivity of CeOs<sub>4</sub>Sb<sub>12</sub> shows a strongly temperature dependent response with a pronounced peak at 70 meV below 160 K, and a weak shoulder at 30 meV below 60 K [63, 64]. This behaviour of the conductivity of CeOs<sub>4</sub>Sb<sub>12</sub> was attributed to an opening of the charge gaps in the strongly hybridized band near  $E_F$ . The peak at 70 meV was interpreted in terms of an optical excitation across the direct gap with a momentum conserving ( $\partial Q = 0$ ) dipole allowed transition between the two hybridized bands. On the other hand, the origin of the weak shoulder at 30 meV was tentatively attributed to an optically forbidden transition ( $\partial Q \neq 0$ ), which might be allowed with a weak intensity in the presence of defects or an impurity [63, 64]. The key question regarding the charge gap feature found in CeOs<sub>4</sub>Sb<sub>12</sub> is whether it is somehow connected to the spin degrees of freedom. Furthermore, it would be interesting to understand the origin of 30 meV peak in the optical study and the nature of the  $4f$ -electrons in CeOs<sub>4</sub>Sb<sub>12</sub>. Inelastic neutron scattering is an ideal technique for a detailed investigation of the observed features at 30 and 70 meV in the optical study of CeOs<sub>4</sub>Sb<sub>12</sub>. Here we present a brief summary of our inelastic neutron scattering study on CeOs<sub>4</sub>Sb<sub>12</sub> and the detailed results have been reported in ref. [53].

#### 3.2.2 Inelastic neutron scattering study: Evidence of two spin gaps

Inelastic neutron scattering measurements on CeOs<sub>4</sub>Sb<sub>12</sub> and on the nonmagnetic reference compound LaOs<sub>4</sub>Sb<sub>12</sub> were carried out using the time-of-flight chopper spectrometer HET at ISIS facility, with incident neutron energies  $E_i = 23$  and  $200 \text{ meV}$  at 5 and 176 K. Fig.7 shows the estimated magnetic scattering from CeOs<sub>4</sub>Sb<sub>12</sub> at 5 and 176 K with  $E_i = 23 \text{ meV}$ . It is clear from Fig.7 that there is no magnetic scattering at 5 K, while at 176 K we can see a clear presence of quasi-elastic scattering. The absence of magnetic scattering at 5 K in CeOs<sub>4</sub>Sb<sub>12</sub> demonstrates the spin gap formation near  $E_F$ . Further at 176 K the magnetic response exhibits a quasi-elastic scattering, which is very similar to that observed in CeRu<sub>4</sub>Sb<sub>12</sub> and Ce<sub>3</sub>Bi<sub>4</sub>Pt<sub>3</sub>. The observed low energy magnetic response in CeOs<sub>4</sub>Sb<sub>12</sub> seems to be in agreement with the temperature dependent response observed in the optical study and indicates the presence of a spin gap [63].

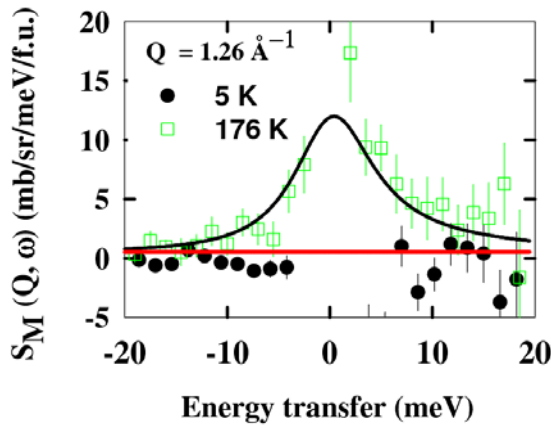


Fig. 7. (color online) Magnetic scattering from  $CeOs_4Sb_{12}$  at 5 and 176 K, measured with  $E_i=23$  meV [53]. The solid line represents the fit to a Lorentzian function.

Fig. 8 shows the estimated magnetic scattering in  $CeOs_4Sb_{12}$  by subtracting off the phonon contribution using the  $LaOs_4Sb_{12}$  data with  $E_i = 200$  meV at 5 K. The inset shows clearly that the magnetic scattering is greater at 5 K than at 176 K. The vertical arrows indicate the position of the charge gaps observed in the optical study [63]. At 5 K, the magnetic scattering has a peak around 27 meV and extends as high as 80 meV. Furthermore, the estimated magnetic scattering at 176 K shows similar behaviour, but with a much reduced intensity between 25 and 80 meV (Inset Fig. 8). Again the Q-dependence of the energy integrated intensity between 30 and 75 meV follows, as expected, the square of the  $Ce^{3+}$  magnetic form factor.

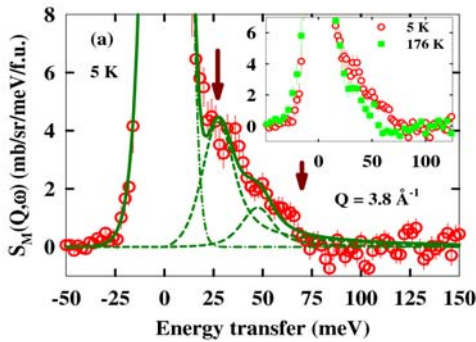


Fig. 8. (color online) The estimated magnetic scattering of  $CeOs_4Sb_{12}$  at 5K after subtracting the scattering from  $LaOs_4Sb_{12}$  (see text) [53]. The solid and dash lines represent the fit using two Lorentzian functions (see text). The inset shows the magnetic scattering at 5 and 176 K for comparison.

The analysis of the magnetic scattering data at 5 K taken with  $E_i = 200$  meV was carried out using a single Lorentzian function convoluted with the instrument resolution function (fit not shown here). However, this approach did not give a good fit to the data between 40 and 80 meV. Thus two Lorentzian functions were used to

fit the data, which improve the fit in this energy range (see Fig. 8, where the solid line represents the fit and the dash lines represent the components of the fit), and yields peaks centred at 27(2) and 48(2) meV with linewidth of 5.2 meV for both peaks. The value of  $\chi'(0)$  estimated from the total intensity of these peaks is  $4.0(5) \times 10^{-3}$  emu/mol. This analysis seems to support our claim that there exist two energy gaps in the inelastic response of  $CeOs_4Sb_{12}$ , which is in agreement with the optical study [63].

The two energy scales, 27 and 50-60 meV, seen in our inelastic neutron scattering of  $CeOs_4Sb_{12}$ , are unusual and not commonly observed in spin gap systems. However, we note that two energy scales have been observed in recent studies of polycrystalline  $YbAl_3$  and single crystal studies of  $YbAl_3$  and  $YbB_{12}$  [61, 72, 80-81]. Following the discussions given in these publications, we can interpret the low energy excitation seen at 27 meV as an indirect excitation, with  $\partial Q \neq 0$ , across the hybridized bands, while the higher energy excitation at 50-60 meV may originate from a direct excitation across the hybridized bands with  $\partial Q = 0$ : it is to be noted that due to the kinematic limitation of neutron scattering one cannot have  $\partial Q = 0$  at finite energy transfer. The intensity of inelastic transitions in interband scattering (i.e. indirect and direct transitions) is proportional to the product of the DOS in the initial and final states [61]. As mentioned previously, the theoretical calculations show that the top of the lower band and bottom of the upper band are strongly dominated by  $4f$ -density of states and the remaining part of the bands are dominated by conduction electrons, hence low density of states [3]. Therefore, the intensity of the low energy peak (i.e. the indirect excitation) is expected to be stronger than that of the high energy peak (i.e. the direct excitation). In this scenario, the most intense peak occurs at the threshold value of energy transfer for the indirect transitions from the zone boundary of the lower band to the zone centre of the upper band. Further it is very interesting to note that a recent study of the nuclear-spin relaxation rate  $1/T_1$ , measured using Sb-NQR, of  $CeOs_4Sb_{12}$  showed the presence of a gap  $\Delta_{NMR} = 27.6$  meV [82], which is remarkably similar to the spin gap of 27 meV (low energy gap) found in our neutron scattering studies.

### 3.3 $CeFe_4Sb_{12}$ : Single ion versus intersite interactions

#### 3.3.1 Crystal structure and bulk properties

Recently the cubic compound  $CeFe_4Sb_{12}$  has been extensively investigated using magnetic susceptibility, heat capacity, resistivity, Hall effect,  $^{121}Sb$ -NQR and optical measurements [35, 83-85], which suggest that the physics of this system is reminiscent of that found in  $CeRu_4Sb_{12}$  and  $CeOs_4Sb_{12}$ , i.e. the opening of a gap near  $E_F$ . The transport gap of 50 meV deduced from the Hall effect experiments agrees very well with the peak observed in the optical conductivity at 50 meV in  $CeFe_4Sb_{12}$  [64, 83]. Further the magnetic contribution to the heat capacity exhibits a Schottky-type anomaly with a maximum close to 125 K. The analysis of the heat

capacity data based on the phenomenological model given by Riseborough [3], which considers that the Schottky-type anomaly is due to a hybridization gap (or pseudogap), leads to the gap value of  $\Delta E = 36$  meV at  $E_F$  [54], that is in agreement with the value estimated through Hall effect and optical measurements [64, 83]. It is to be noted that the analysis of the heat capacity data based on the pure crystal field model did not explain the observed height of the heat capacity [54].

Electronic band structure calculations, using density-functional theory within the local-density approximation (LDA) have been carried out for  $\text{CeFe}_4\text{Sb}_{12}$  and  $\text{CeFe}_4\text{P}_{12}$  [86]. These calculations reveal that both compounds are small band-gap semiconductors, with a gap of 100 and 340 meV, respectively [86]. Further the calculations reveal that the Ce is in a near trivalent state in both compounds and the Ce-4*f* states hybridize strongly with both Fe-3*d* states and Sb (or P) *p* orbitals in the vicinity of the Fermi energy. This calculation reveals that the band gaps are the result of this hybridization. It is known that the LDA tends to underestimate the intra-atomic correlation of Ce 4*f* electrons and hence overestimates the hybridization, one can expect that the calculated band gaps are overestimated rather than underestimated, which is otherwise the usual tendency in the LDA.

### 3.3.2 Inelastic neutron scattering study: Single ion versus inter-site interactions

The inelastic neutron scattering investigations on  $\text{CeFe}_4\text{Sb}_{12}$  and the non-magnetic reference compound  $\text{LaFe}_4\text{Sb}_{12}$  have been carried out at 5 K and 300 K with incident energies  $E_i = 150$  and 250 meV and the detailed results are reported in ref. [54]. The comparison of the scattering between these compounds clearly indicates the presence of magnetic scattering above 40 meV and at 5 K in  $\text{CeFe}_4\text{Sb}_{12}$ . The estimated magnetic scattering in  $\text{CeFe}_4\text{Sb}_{12}$  at 5 and 300 K is shown in Fig.9a&b. Interestingly at 5 K, we can see a broad inelastic peak centred around 50 meV, while at 300 K the magnetic response becomes clearly of the quasi-elastic type. This kind of temperature dependence of the magnetic signal has been observed in other skutterudite compounds such as  $\text{CeRu}_4\text{Sb}_{12}$  [50, 51] and  $\text{CeOs}_4\text{Sb}_{12}$  [53] and also in the Kondo semiconductor  $\text{Ce}_3\text{Bi}_4\text{Pt}_3$  [73] and the metallic Kondo compounds  $\text{YbAl}_3$  [70, 72, 80, 81]. This observed temperature dependence of the inelastic response is in agreement with the theoretical calculations of the dynamical susceptibility for Kondo insulators [3].

The analysis of the observed broad magnetic response near 50 meV in  $\text{CeFe}_4\text{Sb}_{12}$  at 5 K using a Lorentzian spectral function gave the spin gap energy  $\Delta_{\text{spin}} = 40$  (3) meV, and the linewidth (HWHM) of about 27 (3) meV. On the other hand, at 300 K the response is better fitted with a quasi-elastic peak (centred at zero energy) with a linewidth of 20 (3) meV. It is interesting to compare the value of the susceptibility estimated through inelastic neutron scattering measurements with that determined using a conventional magnetometer. Using the sum rule for the uniform bulk susceptibility,  $\chi'(0) = 2.8(4) \times 10^{-3}$  emu/mole at 5 K and  $2.7(2) \times 10^{-3}$  at 300 K have been estimated [54]. These values are very close to the value of  $2.4 \times 10^{-3}$  emu/mole estimated from the Ce bulk magnetic

susceptibility  $\chi(300$  K). Furthermore a paramagnetic effective moment of  $\mu_{\text{eff}} = 2.3$  (1)  $\mu_B$  at 5 K has been extracted using the sum rule of  $S(Q, \omega)$ , which is in good agreement with that estimated from the bulk susceptibility as discussed previously. The simulation of the inelastic response based on the crystal field model supports the conclusion that the inelastic response in  $\text{CeFe}_4\text{Sb}_{12}$  arises from excitations across the two hybridized bands and is not due to the pure cubic crystal field excitation [54].

Since the neutron scattering results confirm that the spin gap does exist in  $\text{CeFe}_4\text{Sb}_{12}$ , it would be interesting to determine its *Q*-dependence. The contour plot as a function of energy transfer versus  $|Q|$  shown in Fig. 10a for the magnetic scattering in  $\text{CeFe}_4\text{Sb}_{12}$  at 5 K reveals a broad inelastic peak near 50 meV, whose position is nearly independent of *Q*. This may indicate a single ion Kondo type response in agreement with the susceptibility measurements of  $\text{Ce}_{1-x}\text{La}_x\text{Fe}_4\text{Sb}_{12}$  ( $x = 1$  to 0.5), which reveal that the peak in the susceptibility is nearly independent of La-doping [83]. However, the *Q* dependence of the energy integrated intensity between 40 and 65 meV for both the incident energies of 150 and 250 meV exhibits a broad maximum near  $Q \sim 2 \text{ \AA}^{-1}$  (Fig. 10b). This behaviour is different from that observed in  $\text{CeRu}_4\text{Sb}_{12}$  and  $\text{CeOs}_4\text{Sb}_{12}$  and from that expected for the magnetic form factor of  $\text{Ce}^{3+}$ : for comparison purpose the  $\text{Ce}^{3+}$  magnetic form factor squared ( $F^2(Q)$ ) has also been plotted in Fig. 10b (solid line).

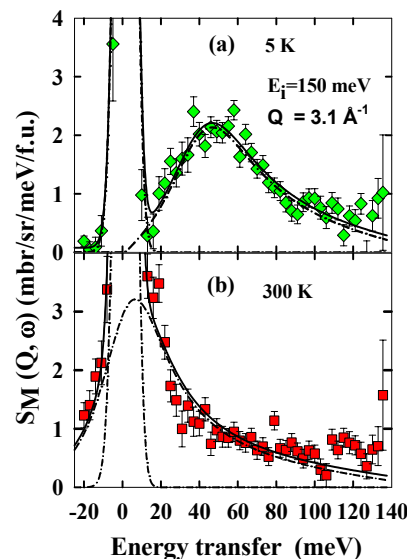


Fig. 9. (color online) Inelastic neutron scattering spectra showing the Ce magnetic response for  $\text{CeFe}_4\text{Sb}_{12}$  at 5 and 300 K after subtraction off the nonmagnetic scattering [54]. The solid line represents the result of the refinement (see the text for details). Dash-dotted lines show the separated contributions of the elastic, inelastic and background signals.

At present there is no clear explanation for the observed *Q*-dependence behaviour of the intensity in  $\text{CeFe}_4\text{Sb}_{12}$  [54]. One of the possibilities is that it may be due to the presence of weak short-range exchange interactions between the Ce and Fe ions. As Ce-Ce distances are larger (7.91 Å) in  $\text{CeFe}_4\text{Sb}_{12}$  as well as the

maximum in the susceptibility of  $\text{Ce}_{1-x}\text{La}_x\text{Fe}_4\text{Sb}_{12}$  is independent of La concentration [83], which furthermore support the single impurity type behaviour of the Ce ions. Thus, it is quite possible that weak inter-site correlations may exist between the Ce and Fe atoms, due to the shorter Ce-Fe distance 3.95 Å as well as to the paramagnetic nature of the Fe ion in  $\text{CeFe}_4\text{Sb}_{12}$ , and most likely responsible for the observed Q-dependence intensity. This interpretation has been supported through the band structure calculations discussed previously, which reveal the presence of strong hybridization between Ce-*4f* and Fe-*3d* electrons. An important role of the Fe ion in  $\text{CeFe}_4\text{Sb}_{12}$  can be seen when we consider the spin gap energy of 40-50 meV, which is relatively larger than that of 30 meV in  $\text{CeRu}_4\text{Sb}_{12}$  and 27 meV in  $\text{CeOs}_4\text{Sb}_{12}$ . This is also true for the Pr-based skutterudite superconductors:  $\text{PrT}_4\text{Sb}_{12}$  (T=Fe, Ru and Os) all having a singlet ground state [87-89]. The Pr compounds with T = Os and Ru are superconducting with  $T_c \sim 1.9$  K and 1 K, respectively, but no superconductivity has been observed in T = Fe compound. This observation again suggests the special role played by the Fe ion in both the Ce and Pr-based skutterudite compounds.

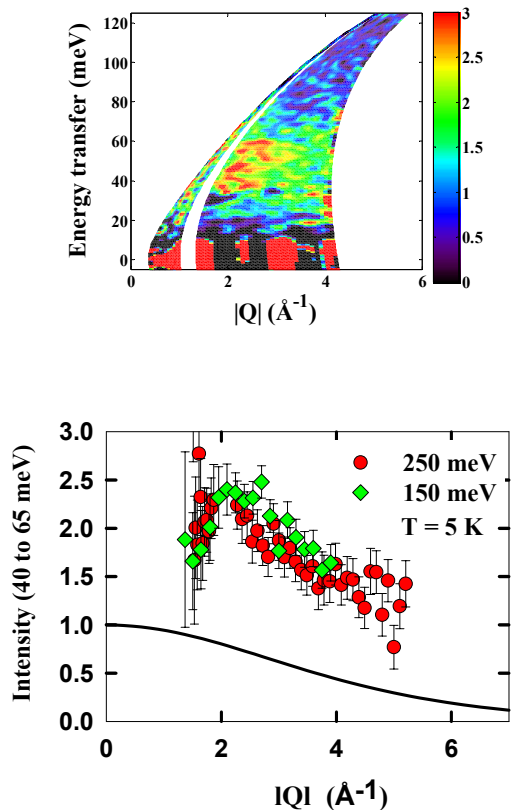


Fig. 10. (color online) (a) Contour map of the magnetic scattering for  $\text{CeFe}_4\text{Sb}_{12}$  at 5 K plotted as a function of energy transfer ( $E$ ) and wave vector transfer  $|Q|$ . The scattering intensity is color-coded, and (b)  $Q$  dependence of the energy integrated intensity between 40 and 65 meV at 5 K for an incident energy of 150 meV (green diamond) and of 250 meV (red circle) [54].

### 3.4 CeRhAs: A large spin gap formation

#### 3.4.1 Crystal structure and bulk properties

The compounds exhibiting spin gap behaviour usually crystallize in a cubic structure [7]. There are only a few non-cubic compounds, which have been reported to show a gap formation at  $E_F$ , for example the orthorhombic  $\text{CeNiSn}$  and  $\text{CeRhSb}$  and the tetragonal  $\text{U}_2\text{Ru}_2\text{Sn}$  and  $\text{U}_2\text{RuGa}_8$  [16, 17, 29, 36]. Interestingly enough,  $\text{CeRhAs}$  is one of such examples that exhibits a gap formation at low temperatures and shows anomalous structural, magnetic, and transport properties below 500 K [27]. At room temperature it crystallizes in the orthorhombic  $\text{TiNiSi}$ -type structure, similar to that of  $\text{CeNiSn}$  and  $\text{CeRhSb}$ , while above  $T_1=360$  K it exhibits a structural transformation to the hexagonal  $\text{LiGaGe}$ -type [27]. Further two additional phase transitions at  $T_2=235$  K and  $T_3=165$  K have been identified by the formation of the superlattice peaks in the x-ray diffraction study as well as anomalies in the resistivity, magnetic susceptibility and heat capacity [27]. The susceptibility exhibits a maximum at  $T_{\text{max}} = 510$  K, below which the gap is believed to open. The temperature dependent resistivity shows strong anisotropy and exhibits step-like anomalies at 360, 235 and 165 K, and increases by two orders of magnitude on cooling to 1.5 K [27].

The gap energy estimated from the transport measurements is  $\Delta_{\text{trans}} = 40\text{-}50$  meV [90], while high-resolution photoemission spectroscopy studies show a gap of  $\Delta_{\text{PES}}=90\text{-}100$  meV [91]. We note that the gap obtained from the photoemission experiment is close to the charge gap of  $\Delta_{\text{char}}=100$  meV estimated from optical study [92]. On the other hand, an NMR study found a much smaller energy gap, i.e. 23 meV [93]. Further the results of the electronic band structure calculations predict that the ground state of  $\text{CeRhAs}$  is insulating with an indirect band gap of 38 meV [94]. Furthermore the electron tunnelling measurements reveal the gap energy of 500 ( $\pm 100$ ) meV at 4 K in  $\text{CeRhAs}$  [90], which is very high compared to that estimated through other techniques mentioned above [91-95]. Thus it is interesting to investigate the magnitude of the spin gap and its  $q$ -dependence in  $\text{CeRhAs}$  through inelastic neutron scattering that gives direct information on the magnitude of the spin gap formation. In the following section, we have summarized our inelastic neutron scattering results on  $\text{CeRhAs}$  and the detailed results are published in ref. [95].

#### 3.4.2 Inelastic neutron scattering study: A large spin gap formation

The inelastic neutron scattering measurements were carried out on a polycrystalline sample of  $\text{CeRhAs}$  with two different neutron incident energies of  $E_i = 23$  and 500 meV at 7 K using the time-of-flight spectrometer HET at ISIS [95]. To estimate correct phonon contributions, we also measured non-magnetic isostructural  $\text{LaRhSb}$  under identical conditions. The observed temperature and momentum dependence of the 23 meV data at 7 K reveal

that there is no additional magnetic scattering in CeRhAs compared with LaRhSb below 20 meV. On the other hand, our higher energy measurements with  $E_i = 500$  meV (Fig. 11a) show clearly that there is an extra scattering between 100 and 400 meV at the low angle ( $4.9^\circ$ ) in CeRhAs compared with that of LaRhSb. Further the estimated magnetic scattering exhibits a broad peak centred near 150 meV and extends up to 400 meV (see Fig. 11c). Therefore, these results indicate that the characteristic energy scale for CeRhAs is 150 meV. Interestingly enough, this energy scale is in good agreement with the broad peak observed at  $\sim 510$  K in the bulk susceptibility with  $T_K = 3 \times T_{\max}(\chi)$  ( $T_K = 1530$  K) according to a single impurity Anderson model [67]. It is to be noted that for  $\text{CeT}_4\text{Sb}_{12}$  ( $T=\text{Ru, Os and Fe}$ ) we found the spin gap energy that agrees well with  $3 \times T_{\max}(\chi)$  [53, 54]. The  $Q$ -dependence of the magnetic intensity, integrated between 120 and 350 meV, follows as expected the theoretical magnetic form factor squared of  $\text{Ce}^{3+}$  ion (inset Fig. 11b). Further, comparison of the spin gap energy of 150 meV with that of charge gap of 100 meV reveals that the spin gap is larger than the charge gap in CeRhAs, which is not the case for  $\text{CeT}_4\text{Sb}_{12}$  ( $T=\text{Ru, Os and Fe}$ ). At present we do not have any clear explanation for this particular behaviour and suggest that more experimental as well as theoretical investigations, especially single crystal neutron studies, are needed to fully understand the gap formation in CeRhAs.

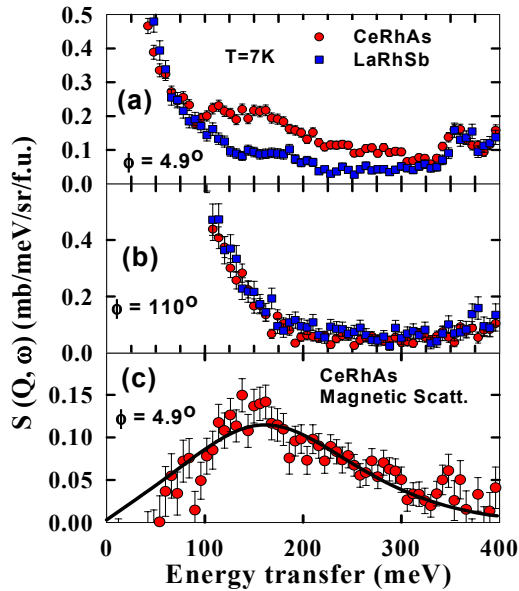


Fig. 11. (color online) Inelastic response from CeRhAs and LaRhSb measured with  $E_i=500$  meV (a) from the low scattering angle ( $4.9^\circ$ ), (b) from the high scattering angle ( $110^\circ$ ), and (c) our estimate of magnetic response for CeRhAs at the low scattering angle. The solid line represents the fit using a Lorentzian function. The inset in (b) shows the  $Q$  dependence of the inelastic peak intensity integrated from 120 to 350 meV (symbols) and the solid line represents the square of the theoretical  $\text{Ce}^{3+}$  magnetic form factor

## 4.5 $\text{U}_{2-x}\text{Th}_x\text{Ru}_2\text{Sn}$ : Kondo lattice effect in the spin gap formation

### 4.5.1 Crystal structure and bulk properties

$\text{U}_2\text{Ru}_2\text{Sn}$  crystallizes in the tetragonal  $\text{Mo}_2\text{FeB}_2$ -type structure [96], an ordered derivative of the  $\text{U}_3\text{Si}_2$ -type structure, with space group  $P4/\text{mbm}$  (number 127) (see Fig.12). It is worth emphasising the distinct layer-type crystal structure of this compound that provides a unique possibility for the 2D nature of magnetic exchange interactions between the U-U atoms. The layers are composed of two different alternating atomic layers, one containing only U atoms and the other one with Ru and Sn atoms. The U-U distance in the a-b plane is 3.920 Å and parallel to c-axis is 3.563 Å. In  $\text{U}_2\text{T}_2\text{X}$  compounds, the shortest U-U links are found either in the basal plane or along the c-axis depending on the choice of the constituent elements. Theoretical studies explain some of the unusual properties of  $\text{U}_2\text{T}_2\text{X}$  ( $T = \text{transition metals and X}=\text{Sn and In}$ ) compounds as being due to strong hybridization between the  $f$ -electrons of U atoms and the  $d$ -electrons of the transition metals [97].

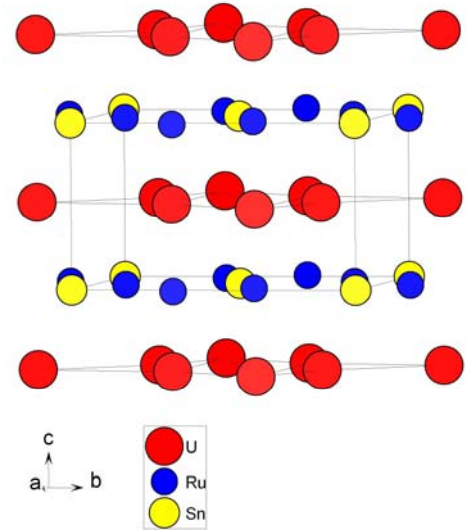


Fig. 12. (color online) The tetragonal unit cell of  $\text{U}_2\text{Ru}_2\text{Sn}$ .

The first resistivity study of  $\text{U}_2\text{Ru}_2\text{Sn}$  revealed semiconducting behaviour below 40 K,  $-\log(T)$  behaviour at high temperatures and a drop below 100 K due to an onset of coherence in the Kondo lattice [29]. These observations suggest the Kondo insulator or semimetal type ground state with a transport energy gap of 1.43 (1) K at  $E_F$  in  $\text{U}_2\text{Ru}_2\text{Sn}$  [29]. Further support of a gap formation comes from the specific heat, magnetoresistance, Hall coefficient, thermal conductivity, thermoelectric power, and  $^{119}\text{Sn}$  NMR measurements on  $\text{U}_2\text{Ru}_2\text{Sn}$  [98-102]. The estimated energy gap in  $\text{U}_2\text{Ru}_2\text{Sn}$  from the specific heat and the first NMR measurements is

approximately of 160 K [100, 102]. However, from recent  $^{119}\text{Sn}$  NMR measurements, Rajarajan *et al.* [103] have obtained the gap of 230 K. Further the Knight shifts (KS) exhibit strong anisotropy that increases at low temperatures with a maximum at 230 K ( $c//H$ ) and 250 K ( $c\perp H$ ). Electronic band structure calculations have been carried out for  $\text{U}_2\text{Ru}_2\text{Sn}$  [104] by tight binding LMTO method that also lead to a pseudogap at  $E_F$ , with a finite DOS indicating a semimetallic character. Further the DOS in the vicinity of the Fermi energy shows a V-shaped pseudogap at about 40 meV below the Fermi level [104]. The susceptibility measurements on polycrystalline  $\text{U}_2\text{Ru}_2\text{Sn}$  revealed a distinct maximum in the susceptibility near temperature 170 K [99], while the presence of strong anisotropy is evidenced in the single crystal susceptibility measured for both directions  $a$  and  $c$ , which passes through a broad maximum at temperatures around 170 or 190 K, respectively (see Fig.13) [102, 105].

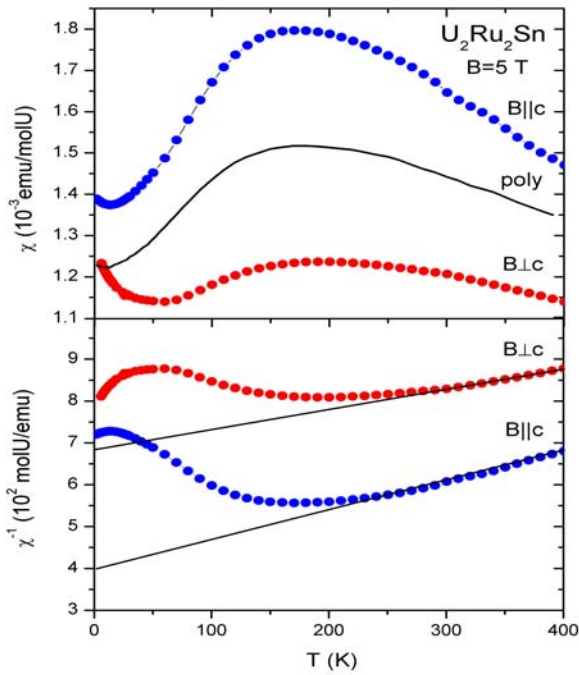


Fig. 13. (color online) Temperature dependences of magnetic susceptibility and the inverse susceptibility of single crystalline  $\text{U}_2\text{Ru}_2\text{Sn}$  along the  $c$  and  $a$  axes (from R. Troć [105]).

Furthermore it is interesting to mention here the effect of Th substitution for U in  $\text{U}_2\text{Ru}_2\text{Sn}$  on the bulk properties [106]. The magnetic susceptibility and resistivity of  $(\text{U}_{1-x}\text{Th}_x)_2\text{Ru}_2\text{Sn}$  ( $x=0$  to 0.2) change dramatically with Th-doping. The maximum in the susceptibility near 170-190 K becomes less pronounced and the low temperature susceptibility exhibits a considerable increase with the Th-doping. For  $(\text{U}_{0.8}\text{Th}_{0.2})_2\text{Ru}_2\text{Sn}$  the high temperature susceptibility exhibits Curie-Weiss behaviour and deviates considerably from it below 100 K [106]. The resistivity of this sample shows a very weak temperature dependence

between 4 and 300 K. The effect of Th doping in  $\text{U}_2\text{Ru}_2\text{Sn}$  clearly reveals that the U-lattice (i.e. Kondo lattice) is playing an important role in the physical properties of this compound, which is not the case in  $\text{Ce}_{1-x}\text{La}_x\text{Ru}_4\text{Sb}_{12}$  and  $\text{Ce}_{1-x}\text{La}_x\text{Fe}_4\text{Sb}_{12}$ . Thus in order to understand the nature of the  $5f$ -electronic state and the role of Kondo lattice in the gap formation, we have carried out inelastic neutron scattering measurements on  $\text{U}_2\text{Ru}_2\text{Sn}$  and  $(\text{U}_{0.8}\text{Th}_{0.2})_2\text{Ru}_2\text{Sn}$  and the results are discussed below: the detailed results will be published elsewhere [107].

#### 4.5.2 Inelastic neutron scattering study: Kondo lattice effect in the spin gap formation

The inelastic neutron scattering measurements were carried out on polycrystalline samples of  $\text{U}_2\text{Ru}_2\text{Sn}$  and  $(\text{U}_{0.8}\text{Th}_{0.2})_2\text{Ru}_2\text{Sn}$  on the HET spectrometer at ISIS with an incident neutron energy of 250 meV at 7 K. A non-magnetic phonon reference sample  $\text{Th}_2\text{Ru}_2\text{Sn}$  was also measured under identical conditions in order to subtract the phonon background from the observed total inelastic response of  $\text{U}_2\text{Ru}_2\text{Sn}$  and  $(\text{U}_{0.8}\text{Th}_{0.2})_2\text{Ru}_2\text{Sn}$ . Fig. 14a & b show the estimated magnetic response after subtracting off the phonon signal in these compounds. It is clear from Fig. 14a that the magnetic response increases above 25 meV and exhibits a broad peak near 70 meV. Further the magnetic response extends up to 240 meV. The absence of a magnetic response below 25 meV was also confirmed from our low energy measurements (data not shown here). The observed magnetic response indicates the formation of a spin gap in  $\text{U}_2\text{Ru}_2\text{Sn}$  near  $E_F$ . As discussed in the previous spin gaps systems:  $\text{CeT}_4\text{Sb}_{12}$  and  $\text{CeRhAs}$ , we can take the peak position as a measure of the spin gap value in  $\text{U}_2\text{Ru}_2\text{Sn}$  that gives the spin gap value of 81(3) meV at 7 K. This value is significantly higher than the 20 meV (230 K) estimated from the recent NMR measurements [103] and much higher than that estimated from the heat capacity measurements, 14 meV (160 K) [100, 101]. As shown by Adroja *et al.* [53] and also discussed below in the next section, there is a universal scaling relation between the spin gap energy and the Kondo temperature,  $T_K = 3 \times T_{\text{max}}(\chi)$ . If we take the peak position of the susceptibility at 190 K (for the single crystal  $B//c$ -axis, which is an easy axis) then this gives a spin gap of 50 meV [105]. However, the estimated spin gap from the inelastic peak position is higher than that predicted using the susceptibility peak, but close to that  $3 \times T_{\text{max}}^{\text{KS}}$ , where  $T_{\text{max}}^{\text{KS}}$  is the temperature where KS exhibits a maximum. At present we do not have any clear explanation for this discrepancy, but one of the reasons could be the presence of strongly anisotropic hybridization, which results into a wave vector dependence gap and hence a single crystal neutron scattering study is high desirable. It would also be interesting to investigate the charge gap in  $\text{U}_2\text{Ru}_2\text{Sn}$  by an optical study and make a direct comparison with the observed spin gap. This might throw some light on the observed discrepancy between the spin gap and the susceptibility maximum. Interestingly, when we compare the magnetic response of  $(\text{U}_{0.8}\text{Th}_{0.2})_2\text{Ru}_2\text{Sn}$  with that of

$U_2Ru_2Sn$  it is clear that the magnetic response has moved to lower energy and there is a strong quasi-elastic scattering presence in the former (see Fig. 14a & b). These observations are in agreement with the temperature dependence of the susceptibility and resistivity and may suggest that the spin gap has collapsed (or renormalized dramatically) in  $(U_{0.8}Th_{0.2})_2Ru_2Sn$ , indicating that the Kondo lattice effect is playing an important role in the spin gap formation in  $U_2Ru_2Sn$ .

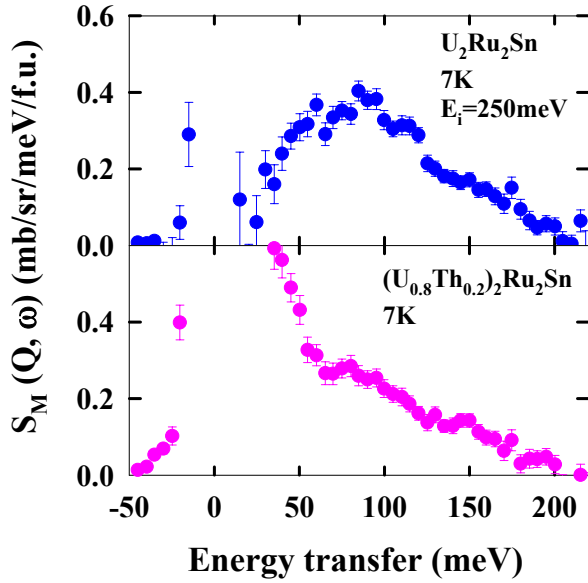


Fig.14. (color online) Inelastic magnetic response after subtracting the phonon background from (a)  $U_2Ru_2Sn$  and, (b)  $(U_{0.8}Th_{0.2})_2Ru_2Sn$  for the low scattering angle ( $19^\circ$ ) at 7 K.

## 5. Comparison between the spin gap and charge gap

It is interesting to compare the absolute value of the spin gap energy estimated from the inelastic neutron scattering measurements with that of the charge gap estimated through the optical studies, and to compare the ratio between these two gaps with the theoretical predictions [20, 74, 108-109]. In Table-1 we have given the value of the spin gap, estimated from the inelastic neutron scattering, the charge gap estimated from the optical study, and the ratio of the spin gap and charge gap for the systems investigated in the present work along with many other Kondo insulators or mixed-valence systems for comparison purposes. It is clear from Table-1 that for  $CeT_4Sb_{12}$  ( $T=Ru, Fe$  and  $Os$ ) the spin gap is smaller than the charge gap and the ratio of the spin gap to charge gap varies from 0.64 to 0.9. It is to be noticed that the absolute value of the spin gap of 40 meV observed in  $CeFe_4Sb_{12}$  is larger than the spin gap value of 30 meV and 27 meV observed in  $CeRu_4Sb_{12}$  and  $CeOs_4Sb_{12}$ , respectively, which indicates the presence of stronger hybridization in the former compound. Further, Table-1 reveals that for  $YbAl_3$  and  $CeNiSn$  the value of the spin gap is much smaller than

that of the charge gap and the ratio is close to 0.33. The theoretically predicted value of this ratio for the infinite dimensional Anderson lattice model is 0.3-0.4 [74, 91] and for the 1-dimension Anderson lattice mode is to 0.7-0.9 [20, 91, 108]. Further it has been shown that for the one-dimensional (1D) Kondo lattice model at half-filling the charge gap is greater than the spin gap for all value of coupling strengths ( $J_{sf}$ ) [109]. The ratio of the spin gap to charge gap is very much depends on the strength of  $J_{sf}$ : for  $J_{sf} \sim 2-4$  the ratio is 0.7-0.73 [109]. Furthermore the model based on Wigner crystallization of electrons proposed by Kasuya et al [110] reveals that the spin and charge gaps have the same magnitude [110]. Since the mechanism of gap formation in this model originates in a charge density wave at low temperature, the resultant partial DOS is expected to have almost the same shape for both f and conduction electrons. On the other hand, the ratio of 1.5 estimated for  $CeRhAs$  is high compared with that estimated for other systems mentioned here and also with the theoretical predictions. Further optical study on  $U_2Ru_2Sn$  is very important to understand the high value of the spin gap in this compound.

Table 1. Magnitude of the Spin and charge gaps in heavy fermion systems.

System	Spin gap(meV)	Charge gap (meV)	Spin/Char
$CeRu_4Sb_{12}$	30	47	0.64
$CeFe_4Sb_{12}$	40	50	0.8
$CeOs_4Sb_{12}$	27 & 50	30 & 70	0.7-0.9
$YbAl_3$	30	100	0.30
$Ce_3Bi_4Pt_3$	21.5	38.8	0.55
$CeNiSn$	2-4.5	10	$\sim 0.33$
$YbB_{12}$	14	25	0.56
$CeRhAs$	150	$\sim 100$	1.5
$U_2Ru_2Sn$	70	?	?
$CeRhSn$	20-30	?	?

Rozenberg *et al.* [74] have calculated the local spin-spin susceptibility (related to the spin gap) and charge-charge susceptibility (related to the charge gap) as well as the optical conductivity of the periodic Anderson model in their dynamical mean-field theory. The results of their calculations are presented in Fig. 15b. For comparison, we have also plotted the inelastic neutron scattering response and optical conductivity of  $CeRu_4Sb_{12}$  in Fig. 15a. The comparison between theoretical and experimental results reveals very similar behaviour. Further the dependence of the spin gap and the charge gap on the Coulomb interaction  $U$  is shown in the inset of Fig. 15b. According to this calculation, the Coulomb interaction  $U$  reduces the hybridization from its bare value  $V$  to a renormalized value  $V^*$ , which decreases as  $U$  increases. As a consequence, the charge gap in the optical conductivity decreases faster than the spin gap with increasing  $U$  [74]. It is interesting to mention here that the gap in  $Ce_{1-x}La_xRu_2Sb_{12}$  (evidence from the neutron scattering results) as well as in  $Ce_{1-x}La_xFe_2Sb_{12}$  and  $Ce_{1-x}La_xOs_2Sb_{12}$  (evidence from the peak

position in the susceptibility) seems to be independent of La-doping, which may suggest that the Coulomb interaction and hence the hybridization do not change much with the La-doping.

## 6. Universal scaling relation between the spin gap energy and Kondo temperature

Adroja *et al.* [53] have reported that there exists a universal scaling between the spin gap energy estimated through the inelastic neutron scattering and the Kondo temperature estimated from the peak position of the temperature dependence of the susceptibility. Further, this scaling was also applied to a wider range of compounds by Viennois *et al.* [54], who have shown that very similar scaling behaviour exists between the spin gap energy and the associated anomalies in the heat capacity or thermal expansion for a series of Ce and Yb-based compounds.

temperature Kondo temperature associated with the full degeneracy for the scaling analysis. According to the single impurity model [67], we can estimate the high temperature Kondo temperature  $T_K$  through the maximum  $T_{\max}(\chi)$  in the bulk susceptibility as  $T_K = 3 \times T_{\max}(\chi)$ . Therefore it would be interesting to show a universal relation between the inelastic peak position (or spin gap energy) and the high temperature Kondo temperature  $T_K$  or  $T_{\max}(\chi)$ , as shown in refs. [53, 54]. In Fig.16 we have plotted the peak position of the inelastic neutron scattering versus  $T_K$  (or  $3 \times T_{\max}(\chi)$ ) for many Ce and Yb based intermediate valence compounds. We can see that the excellent universal scaling relation is observed between  $T_K$  or  $T_{\max}(\chi)$  and the inelastic peak position corresponding to the spin gap in all these compounds, notably for the case of three different  $CeM_4Sb_{12}$  ( $M=Fe, Ru$  and  $Os$ ) skutterudite compounds and  $CeRhAs$ . As we mentioned previously the value of spin gap in  $U_2Ru_2Sn$  is higher than that expected from the universal scaling discussed here and we need further investigation to understand this behaviour.

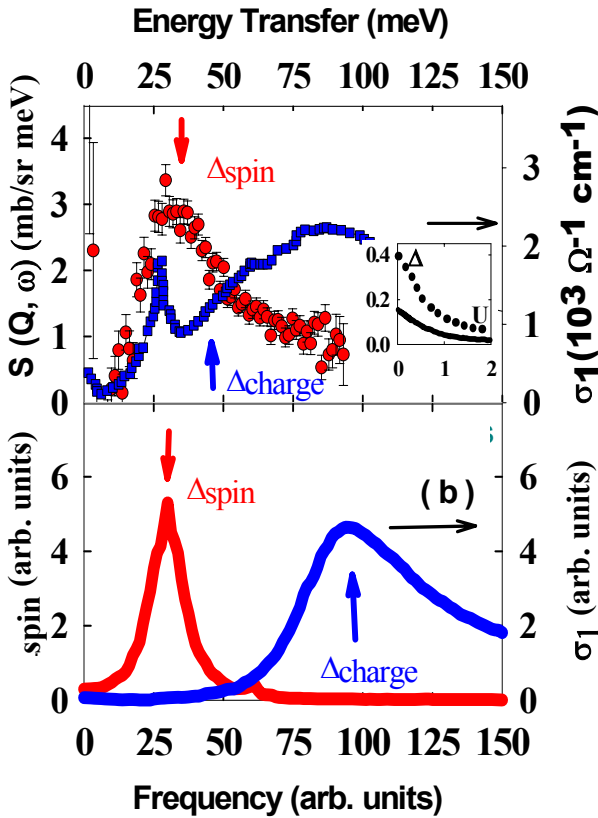


Fig. 15 (color online) (a) Inelastic neutron scattering response and optical conductivity (from ref. 62) of  $CeRu_4Sb_{12}$ , and (b) the local spin-spin susceptibility and optical conductivity calculated for the periodic Anderson model within the dynamical mean-field theory with the parameters Coulomb interaction  $U=1$  and hybridization  $V=0.2$  from Rozenberg *et al.* [74]. The inset shows the variation of the charge (or indirect) gap (dotted line) and spin gap (solid line) as a function of Coulomb interaction  $U$  with  $V=0.2$  [74].

It is well known that for mixed valence systems one deals with the full degeneracy  $J=5/2$  ( $7/2$ ) of the  $4f$ -electron for Ce (Yb), which means one can use the high

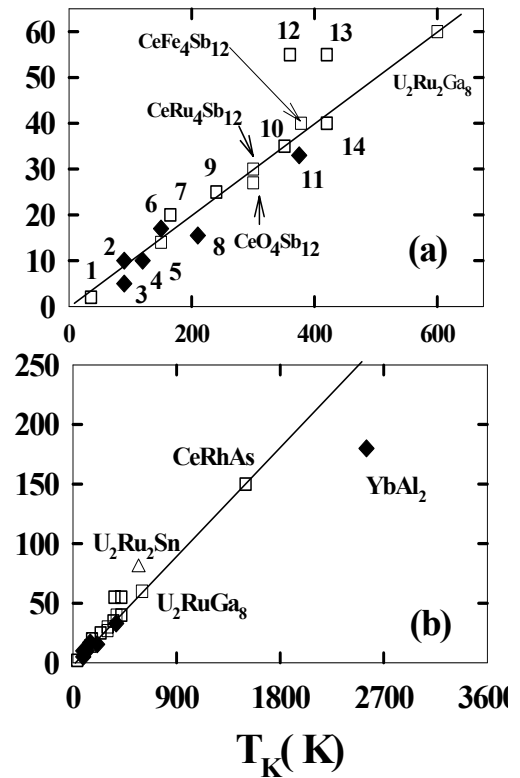


Fig. 16 (a-b) Peak position ( $E_{INS}$ ) in the inelastic neutron scattering (INS) vs. Kondo temperature estimated from the maximum of the magnetic susceptibility ( $T_K=3 \times T_{\max}(\chi)$ ) in the intermediate valence systems and Kondo semiconductors [54]. 1:  $CeNiSn$ ; 2:  $YbCuAl$ ; 3:  $YbPd_2Si_2$ ; 4:  $YbCu_2Si_2$ ; 5:  $SmB_6$ ; 6:  $YbCu_4Ag$ ; 7:  $CePt_2Si_2$ ; 8:  $YbB_{12}$ ; 9:  $Ce_3Bi_4Pt_3$ ; 10:  $CeRhSb$ ; 11:  $YbAl_3$ ; 12:  $CePd_3$ ; 13:  $CeNi$ ; 14:  $CeSn_3$ ; 15:  $U_2RuGa_8$ ; 16:  $U_2Ru_2Sn$ . The solid line is a guide to the eyes. The symbols used in Fig. 16b have same meaning as in Fig. 16a

## 7. Conclusions and further work

We have carried out a systematic investigation of the spin gap formation in  $\text{CeT}_4\text{Sb}_{12}$  ( $T=\text{Ru, Os and Fe}$ ),  $\text{CeRhAs}$  and  $\text{U}_2\text{Ru}_2\text{Sn}$  compounds using inelastic neutron scattering measurements. We have found clear evidence of spin gap formation in these systems. Further our inelastic neutron scattering studies on  $\text{CeOs}_4\text{Sb}_{12}$  reveals the presence of two spin gaps, which is in agreement with that observed through the optical study. Our magnetic susceptibility and inelastic neutron scattering measurements on  $\text{Ce}_{1-x}\text{La}_x\text{Ru}_4\text{Sb}_{12}$  ( $x=0-0.50$ ) reveal that the spin gap in this system is independent of La-doping, suggesting single ion Kondo interactions are responsible for the spin gap formation. Further, the susceptibility of  $\text{Ce}_{1-x}\text{La}_x\text{Fe}_4\text{Sb}_{12}$  ( $x=0-0.8$ ) also exhibits a peak, independent of La-doping, which may suggest that the spin gap formation in this system is also mainly due to single ion nature, and is independent of La-doping, despite that the magnetic intensity exhibits a peak near  $Q = 2 \text{ \AA}^{-1}$ . Inelastic neutron scattering investigations on  $\text{Ce}_{1-x}\text{La}_x\text{Fe}_4\text{Sb}_{12}$  would be highly important to confirm the single ion nature of the spin gap in this system. We mention here that inelastic neutron scattering investigations on  $\text{Ce}_y\text{Fe}_{2.75}\text{Ni}_{1.25}\text{Sb}_{12}$  ( $y=0.5$ ) clearly show that the spin gap collapses with Ni-doping and the system exhibits a well-defined cubic crystal field excitation with an overall CF-splitting of 5 meV [55]. This result suggests that hybridization between Ce- $4f$  and Fe- $3d$  (or Ru- $4d$  in  $T = \text{Ru}$  compound) is important for the gap formation, in agreement with the band structure calculations.

Surprisingly, the temperature dependence of the susceptibility and inelastic neutron scattering response of Th-doped  $\text{U}_2\text{Ru}_2\text{Sn}$  reveals a dramatic change with the doping, which indicates that the spin gap in  $\text{U}_2\text{Ru}_2\text{Sn}$  arises from the Kondo lattice effect. Further, the magnitude of the spin gap (70 meV) in  $\text{U}_2\text{Ru}_2\text{Sn}$  estimated from the inelastic neutron scattering is higher than that estimated through the heat capacity and  $^{121}\text{Sn}$  NMR measurements, which may be due to strong anisotropic hybridization as evidenced through the single crystal susceptibility measurements. It is important to investigate the charge gap in  $\text{U}_2\text{Ru}_2\text{Sn}$  using optical study and compare its magnitude with that of the spin gap. Further, we have discussed the universal scaling relation between the spin gap and the Kondo temperature and presented a comparison between the spin gap and charge gap magnitudes for many strongly correlated electron systems.

## Acknowledgements

We acknowledge our fruitful collaboration with E.A. Goremychkin, R. Osborn, B.D. Rainford, J. Taylor and H. Walker on inelastic neutron scattering (INS) investigations on  $\text{CeOs}_4\text{Sb}_{12}$  and R. Viennois, L.C. Chapon, L. Girard, R. I. Bewley and S. Paschen on the INS study of  $\text{CeFe}_4\text{Sb}_{12}$ . We also thank R.I. Bewley for his help during the inelastic neutron scattering measurements on  $\text{U}_2\text{Ru}_2\text{Sn}$ . We are grateful to A.P. Murani and A. Strydom for stimulating

discussions and the ISIS Facility for providing the beam time and financial support. We thank D. Fort for providing us with  $(\text{U}_{1-x}\text{Th}_x)_2\text{Ru}_2\text{Sn}$  samples, R. Troc for giving permission to show single crystal susceptibility data of  $\text{U}_2\text{Ru}_2\text{Sn}$  and W. Kockelmann for preparing Fig. 12.

## References

- [1] C.M. Varma, *Rev. Mod. Phys.* **48**, 219 (1976).
- [2] A. Georges, G. Kotliar, W. Krauth, M. J. Rozenberg, *Rev. Mod. Phys.* **68**, 13 (1996).
- [3] P.S. Riseborough, *Adv. Phys.* **49**, 257 (2000); P.S. Riseborough, *Phys. Rev. B* **45**, 13984 (1992).
- [4] P. Coleman, *Cond-mat/0612006 V1* (2006).
- [5] G. R. Stewart, *Rev. Mod. Phys.* **73**, 797 (2001); A. Amato, *Rev. Mod. Phys.* **69**, 1119 (1997).
- [6] K. Takegahara, H. Harima, Y. Kaneta, A. Yanase, *J. Phys. Soci. Jpn.* **62**, 2103 (1993); L.F. Matheiss, D.R. Hamman, *Phys. Rev. B* **47**, 13114 (1993).
- [7] G. Aeppli, Z. Fisk, *Comments Cond. Mat. Phys.* **16**, 155 (1992).
- [8] L. Degiorgi, *Rev. Mod. Phys.* **71**, 687 (1999).
- [9] M. Jarrell, H. Akhlaghpour, and Th. Pruschke, *Phys. Rev. Lett.* **70**, 1670 (1993).
- [10] J. Moreno, P. Coleman, *Phys. Rev. Lett.* **84**, 342 (2000).
- [11] K. Hanzawa, *J. Phys. Soc. Jpn.* **71**, 1481 (2002).
- [12] V. Jaccarino, G. K. Wertheim, J. H. Wernick, C. R. Walker, S. Arajs, *Phys. Rev.* **160**, 476 (1967).
- [13] J.C. Cooley, M.C. Aronson, Z. Fisk, P.C. Canfield, *Phys. Rev. Lett.* **74**, 1629 (1995); A.P. Alekseev et al, *J. Phys.: Cond. Matter* **7**, 289 (1995); P.A. Alekseev, V.N. Lazukov, R. Osborn, B.D. Rainford, I.P. Sadikov, E.S. Konovalova and Yu.B. Pederno, *Europhys. Lett.* **23** 347 (1993); For theoretical model, see P.S. Riseborough, *Annalen der Physik* **9**, 813 (2000).
- [14] M. Kasaya, F. Iga, K. Negishi, S. Nakai, T Kasuya, *J. Magn. Magn. Mater.* **31-34**, 437 (1983); K.S. Nemkovski, J.-M. Mignot, A.P. Alekseev, A.S. Ivanov, E.V. Nefedova, A.V. Rybina, L.P. Regnault, F. Iga, and T. Takabatake, *Phys Rev Lett.* **99**, 137204 (2007); A. Bouvet, T. Kasuya, M. Bonnet, L.P. Regnault, J. Rossat-Mignod, F. Iga, B. Fåk, A. Severing, *J.Phys: Cond. Matter.* **10**, 5667 (1998).
- [15] M. F. Hundley, P. C. Canfield, J.D. Thompson, Z. Fisk, J. M. Lawrence, *Phys. Rev.* **B42**, 6842 (1990).
- [16] T. Takabatake, F. Teshina, H. Fujii, S. Nishigori, T. Suzuki, T. Fujita, T. Yamaguchi, J. Sakurai, D. Jaccard, *Phys. Reb.* **B41**, 9607 (1990).
- [17] S.K. Malik, D.T. Adroja, *Phys. Rev.* **B43**, 6277 (1991).
- [18] K. Takegahara, H. Harima, Y. Keneta, A. Yanase, *J. Phys. Soc. Jpn.* **62**, 2103 (1993)
- [19] C. Fu, K.P.C.M. Krijn, S. Doniach, *Phys. Rev.* **B49**, 2219 (1994).
- [20] H. Tsunetsugu, M. Sigrist, K. Ueda, *Rev.*

- Mod. Phys. **69**, 809 (1997).
- [21] A. Tsvetlik, and P. Wiegman, Adv. Phys. **32**, 453 (1983); A.M.Tsvetlik, Phys. Rev. Lett. **72**, 10480 (1994).
- [22] M. Kasaya, K. Khtoh, K. Takegahara, Solid State Commun. **78**, 797 (1991); K. Tatcho, M. Kasaya, Physica **B186-188**, 428 (1993); D.T. Adroja, B.D. Rainford, Zakir Hossain, E.A. Goremychkin, R. Nagarajan, L.C. Gupta, C. Godart, Physica B **206-207**, 216 (1995).
- [23] M.S. Torikachvili *et al.*, in Proc. LT-17, ed. H. Eckern (North-Holland, Amsterdam, 1984), p.875; G. Martins, M.S. Torikachvili, K.N. Yang, M.B. Maple R.P. Guertin, J. Appl. Phys., **57**, 3073 (1985); G.B. Martins, M.A. Pires, G.E. Barberise, C. Rettori, and M.S. Torikachvili, Phys. Rev. **B50**, 14822 (1994).
- [24] E.D. Bauer, A. Slebaraski, E.J. Freeman, C. Sirvent, M.B. Maple, J. Phys. Cond. Matter, **13**, 4495 (2001) ; M. Hedo, Y. Uwatoko, H. Sugawara, and H. Sato, Physica **B329-333**, 456 (2003); H. Sugawara, S. Osaki, M. Kobayashi, T. Namiki, S. R. Saha, Y. Aoki, H. Sato, Phys. Rev. **B71**, 125127 (2005).
- [25] I. Shirota, T. Adachi, K. Tachi, S. Todo, K. Nozawa, T. Yagis, M. Kinoshita, J. Phys. Chem. Solids **57**, 211 (1996).
- [26] C. Sekine, N. Hoshia, K. Takeda, T. Yoshida, I. Shirota, K. Matsuhira, M. Wakeshima, Y. Hinatsu, J. Mag. Mater. **310**, 260 (2007); R. E. Baumbach, P. C. Ho, T. A. Sayles, M. B. Maple, R. Wawryk, T. Cichorek, A. Pietraszko, Z. Henkie, J. Phys.: Condens. Matter **20** 075110 (2008).
- [27] T. Sasakawa, T. Suemitsu, T. Takabatake, Y. Bando, K. Umeo, M. H. Jung, M. Sera, T. Suzuki, T. Fujita, M. Nakajima, K. Iwasa, M. Kohgi, Ch. Paul, St. Berger, E. Bauer, Phys. Rev. **B66**, 41103 (2002).
- [28] T. Takabatake, S. Miyata, H. Fujita, Y. Aoki, T. Suzuki, T. Fujita, J. Sakurai and T. Hiraoka, J. Phys. Soc. Jpn. **59**, 4412 (1990); P.C. Canfield, A. Lacerda, J.D. Thompson, G. Sporn, W. P. Beyermann, M.F. Hundley and Z. Fisk, J. Alloys Comp. **181**, 77 (1992).
- [29] L. Menon, P. V. du Plessis, A. M. Strydom, Solid State Commun. **8**, 519 (1998).
- [30] M.S. Torikachvili, C. Rossel, M.W. McElfresh, M. B. Maple, R.P. Guertin and G.P. Meisner, J. Magn. Magn. Mater. **54-57**, 365 (1986) ; H. Nakotte *et al.*, Physica B **259-261**, 280 (1999); S.V. Dordevic *et al.*, Phys. Rev. **B60**, 11321 (1999).
- [31] P. Haen, F. Lapierre, J.M. Mignot and R. Tournier, Phys. Rev. Lett. **43**, 304 (1979).
- [32] H. Boppart, J. Magn. Magn. Mater. **47-48**, 429 (1985).
- [33] T. Palstra, J. Magn. Magn. Mater. **67**, 331 (1992).
- [34] N. Takeda, M. Ishikawa, J. Phys. Soc. Jpn. **69**, 868 (2000) ; N.R. Dilley, E.D. Bauer, M.B. Maple, S. Dordevic, D.N. Basov, F. Freiberger, T.W. Darling, A. Migliori, B.C. Chakoumakos, and B.C. Sales, Phys. Rev. B **61** 4608 (2000)
- [35] D. T. Morelha, G. P. Meisner, J. Appl. Phys. **77**, 3777 (1995).
- [36] R. Troć, Z. Bukowski, C. Sulkowski, J.A. Morkowski, A. Szajek, G. Chelkowska, Physica B **359-361**, 1375 (2005).
- [37] A.M. Strydom, Z. Guo, S. Paschen, R. Viennois, F. Steglich, Physica B **359-361**, 293 (2005); I. Das E.V. Sampathkumaran, Phys. Rev. **B46** 4250 (1992).
- [38] E. Brüning, M. Baenitz, A. Gippius, A. Rajarajan, A. Strydom, S. Paschen, and F. Steglich, March 2005 Korrelationstage Workshop, Dresden (Germany); E.M. Bruning, M. Baenitz, A.A. Gippius, S. Paschen, A.M. Strydom and F. Steglich, Physica **B378-380**, 839 (2006) ;ibid, J. Magn. Magn. Mater. **310**, 393 (2007).
- [39] K. Sengupta, E.V. Sampathkumaran, T. Nakano, M. Hedo, M. Abliz, N. Fujiwara, Y. Uwatoko, S. Rayaprol, K. Shigetoh, T. Takabatake, T. Doert, J.P.F. Jemetio, Phys. Rev. B **70**, 0644406 (2004); M. Abliz, T. Nakano, E.V. Sampathkumaran, J.P.F. Jemetio, T. Doert, M. Hedo, Y. Uwatoko, J. Phys. Soc. Jpn. **74**, 508 (2005)
- [40] E.V. Sampathkumaran, T. Ekino, R.A. Ribeiro, K. Sengupta, T. Nakano, M. Hedo, N. Fujiwara, M. Abliz, Y. Uwatoko, S. Rayaprol, Th. Doert, J.P.F. Jemetio, Physica **B359-361**, 108 (2005).
- [41] M.S. Kim, Y. Echizen, K. Umeo, S. Kobayashi, M. Sera, P.S. Salamakha, O.L. Sologub, T. Takabatake, X. Chen, T. Tayana, T. Sakakibara, M.H. Jung, M.B. Maple, Phys. Rev. **B68** 054416, (2003); P.-C. Ho, V.S. Zapf, A. Slebarski, M.B. Maple, Philos. Mag. **84**, 2119 (2004).
- [42] D.T. Adroja *et al.*, ISIS experimental report (2005) D.T. Adroja *et al.* (unpublished).
- [43] T. Yamasaki *et al.*, Solid State Commun. **119**, 415 (2001) ; Y. Muro, Y. H. Nakamura, T. Kohara, J. Magn. Magn. Mater. **310**, 1038 (2007); Y. Muro, H. Nakamura, T. Kohara, J. Phys. Cond. Matter **18**, 3931 (2006).
- [44] C. J. Leavey, B.D. Rainford, J.R. Stewart, D.T. Adroja, J. Magn. Magn. Mater. **310**, 1041 (2007); *ibid*, Physica **B378-380**, 675 (2006).
- [45] T. Kondo, T. Takeuchi, A. Kaminski, S. Tsuda, S. Shin, Phys. Rev. Lett. **98**, 267004 (2007); T. Timusk, B. Statt, Rep. Prog. Phys. **62**, 61 (1999); V. J. Emery, S.A. Kivelson, Nature (London) **374**, 434 (1995); C.C. Homes, T. Timusk, R. Liang, D.A. Bonn and W.H. Hardy, Phys. Rev. Lett. **71**, 1645 (1993).
- [46] S. D. Wilson, P. Dai, S. Li, S. X. Chi, H. J. Kang, J. W. Lynn, Nature (London) **442**, 59 (2006).
- [47] H. Okamura, T. Watanabe, M. Matsunami, T. Nishihara, N. Tsujii, T. Ebihara, H. Sugawara, H. Sato, Y. Onuki, Y. Isikawa, T. Takabatake and T. Naba, J. Phys. Soc. Jpn. **76**, 23703 (2007).
- [48] M. Dressel, G. Gruner, *Electrodynamics of Solids* (Cambridge University Press, Cambridge, (2002).
- [49] P. Y. Yu and M. Cardona, Fundamentals of Semiconductors (Springer, Berlin, 2001) 3rd ed., Chap. 6.2.; H. Okamura, T. Michizawa, T. Nanba,

- S.Kimura, F.Iga, T. Takabatake, *J. Phys. Soc. Jpn.* **74**, 1954 (2005).
- [50] D.T. Adroja, J.-G. Park, K.A. McEwen, N. Takeda, M. Ishikawa, J.Y. So, *J. Magn. Magn. Mater.* **272-276**, Supp. 1, E21 (2004).
- [51] D. T. Adroja, J.-G. Park, K. A. McEwen, N. Takeda, M. Ishikawa, J.-Y. So, *Phys. Rev. B* **68**, 094425 (2003).
- [52] D. T. Adroja, J.-G. Park, K. A. McEwen, K. Shigetoh, T. Sasakawa, T. Takabatake, and J.-Y. So, *Physica B* **378**, 788 (2006).
- [53] D. T. Adroja, J.-G. Park, E. A. Goremychkin, K. A. McEwen, N. Takeda, B. D. Rainford, K. S. Knight, J. W. Taylor, J. Park, H. C. Walker, R. Osborn, and P. S. Riseborough, *Phys. Rev. B* **75**, 014418 (2007).
- [54] R. Viennois, L. Girard, L. C. Chapon, D. T. Adroja, R. I. Bewley, D. Ravot, Peter. S. Riseborough, and S. Paschen, *Phys. Rev. B* **76**, 174438 (2007).
- [55] D.T. Adroja, L.C. Chapon, L. Girard, A. Haidoux, D. Ravot, J.W. Taylor, unpublished (2008).
- [56] P.W. Anderson, *Phys. Rev.* **124**, 41 (1961); *Valence Fluctuations in Solids*, edited by L.M. Falicov, W. Hanke M.B. Maple (North-Holland, Amsterdam, 1981) P.451.
- [57] P. Nozieres, *J. Low-Temp. Phys.* **17**, 31 (1974).
- [58] P. Nozieres, A. Blandin, *J. Physique* **41**, 193 (1980).
- [59] H. Ikeda, K. Miyake, *J. Phys. Soc. Jpn.* **65**, 1769 (1996).
- [60] S.H. Liu, *Phys. Rev. B* **63**, 115108 (2001).
- [61] A. D. Christianson, J. M. Lawrence, E. A. Goremychkin, R. Osborn, E. D. Bauer, J. L. Sarrao, J. D. Thompson, C. D. Frost, and J. L. Zarestky, *Phys. Rev. Lett.* **96**, 117206 (2006); H. Okumura, T. Michizawa, T. Nanba, and T. Ebhara, *J. Phys. Soc. Jpn.* **73**, 2045 (2004); H. Kuroiwa, Y. Imai, and T. Saso, *J. Phys. Soc. Jpn.* **76**, 124704 (2007).
- [62] S.V. Dordevic, D.N. Basov, N.R. Dilley, E.D. Bauer, M.B. Maple, *Phys. Rev. Lett.* **86**, 684 (2001).
- [63] M. Matsunami, H. Okamura, T. Namba, H. Sugawara, H. Sato, *J. Phys. Soc. Jpn.* **72**, 2722 (2003).
- [64] M. Matsunami, H. Okamura, T. Namba, H. Sugawara, H. Sato, *J. Magn. Magn. Mater.* **272-276**, e41 (2004).
- [65] N. Takeda and M. Ishikawa, *Physica B* **259-261**, 92 (1999); N. Takeda *et al.*, *J. Phys. Soc. Jpn.* **69**, 868 (2000); N. Takeda and M. Ishikawa, *Physica B* **281&282**, 388 (2000); N. Takeda and M. Ishikawa, *J. Phys.: Condens. Matter* **13**, 5971 (2001).
- [66] K. Abe, T.D. Matsuda, H. Sugawara, T. Namiki, Y. Aoki, H. Sato, *Physica B* **312**, 256 (2002).
- [67] N.E. Bickers, D.L. Cox, and J.W. Wilkins, *Phys. Rev. Lett.* **54**, 230 (1985).
- [68] E.D. Bauer, A. Šlebarski, R.P. Dickey, E.J. Freeman, C. Sirvent, V.S. Zapf, N.R. Dilley, and M.B. Maple, *J. Phys.: Cond. Matter* **13**, 5183 (2001).
- [69] S.V. Dordevic, I. K. S. D. Beach, N. Takeda, Y. J. Wang, M. B. Maple, D. N. Basov, *Phys Rev Lett.* **96**, 017403 (2006).
- [70] T. Saso J. Ogura, *Physica B* **186-188**, 372 (1993); *Phys. Rev. B* **75**, 134411 (2007); *J. Electron Spectr. Relat Phenom.* **144-147**, 643 (2005).
- [71] A.J. Fedro S.K. Sinha, in *Valence Fluctuations in Solids*, edited by L.M. Falicov, W. Hanke, and M.B. Maple (North-Holland, Amsterdam, 1981) p. 329.
- [72] A.P. Murani, *Phys. Rev. Lett.* **54**, 1444 (1985); *Phys. Rev. B* **50**, 9882 (1994).
- [73] A. Severing, T. Perring, J.D. Thompson, P.C. Canfield, Z. Fisk, *Physica B* **199 & 200**, 480 (1994); A. Severing, J. D. Thompson, P. C. Canfield, Z. Fisk, P. S. Riseborough, *Phys. Rev. B* **44**, 6832 (1991).
- [74] M.J. Rozenberg, G. Kotliar, and H. Kajueter, *Phys. Rev. B* **54**, 8452 (1996).
- [75] P.S. Riseborough, *Phys. Rev. B* **68**, 235213 (2003).
- [76] C. R. Rotundu and B. Andraka, *Phys. Rev. B* **73**, 144429 (2006).
- [77] J.D. Thompson *et al.*, in: *Transport and Thermal Properties of f-Electron Systems*, edited by H. Fujii, T. Fujita and G. Oomi (Plenum, New York, 1993) p. 35; M.F. Hundely *et al.*, *Phys. Rev. B* **50**, 18142 (1994).
- [78] T. Namiki, Y. Aoki, H. Sugawara, H. Sato, *Acta, Phys. Pol.* **B34**, 1161 (2003).
- [79] C.R. Rotundu, B. Andraka, *Phys. Rev. B* **73**, 144429 (2006).
- [80] J.-M. Mignot, P. A. Alekseev, K. S. Nemkovski, L.-P. Regnault, F. Iga, T. Takabatake, *Phys. Rev. Lett.* **94**, 247204 (2005).
- [81] P.A. Alekseev, J.-M. Mignot, K. S. Nemkovski, E. V. Nefedova, N. Yu. Shitsevalova, Yu. B. Paderno, R. I. Bewley, R. S. Eccleston, E. S. Clementyev, V. N. Lazukov, I. P. Sadikov, and N. N. Tiden, *J. Phys. Condens. Matter*, **16**, 2631 (2004).
- [82] ] M. Yogi, H. Kotegawa, G. Zheng, Y. Kitaoka, S. Ohsaki, H. Sugawara, H. Sato, *J. Phys. Soc. Jpn.* **74**, 1950 (2005).
- [83] R. Viennois, D. Ravot, F. Terki, C. Hernandez, S. Charar, P. Haen, S. Paschen, F. Steglich, *J. Mag. Mag. Mat.* **272-276**, e113 (2004) ; R. Viennois, S. Charar, D. Ravot, A. Mauger, P. Haen, and J. C. Tedenac, *J. Phys.: Cond. Mat.* **18**, 5371 (2006); L. Chapon, D. Ravot, and J.-C. Tedenac, *J. Alloys Comp.* **282**, 58 (1999).
- [84] M. E. Danebrock, C. B. H. Evers, and W. Jeischko, *J. Phys. Chem. Solids* **57**, 381 (1996); G. P. Meisner D. T. Morelli, *J. Appl. Phys.* **77**, 3777 (1995) ; D. A. Gajewski, N. R. Dilley, E. D. Bauer, E. J. Freeman, R. Chau, M. B. Maple, D. Mandrus, B. C. Sales, and A. Lacerda, *J. Phys. : Cond. Mat.* **10**, 6973 (1998).
- [85] K. Magishi, H. Sugawara, I. Mori, T. Saito, and K. Koyama, *J. Phys. Chem. Solids* **68**, 2076 (2007).
- [86] L. Nordström, D.J. Singh, *Phys. Rev. B* **53**, 1103 (1996).
- [87] E. A. Goremychkin, R. Osborn, E. D. Bauer, M. B. Maple, N. A. Frederick, W. M. Yuhasz, F. M. Woodward and J. W. Lynn, *Phys. Rev. Lett.* **93**, 157003 (2004).
- [88] D. T. Adroja, J.-G. Park, E.A. Goremychkin, N. Takeda, M. Ishikawa, K.A. McEwen, R. Osborn, A.D. Hillier, and B.D. Rainford, *Physica*

- B **359**, 983 (2005); D. T. Adroja *et al.*, to be published.
- [89] E. Bauer, A. Grytsiv, P. Rogl, W. Kockelmann, A.D. Hillier, E.A. Goremychkin, D.T. Adroja, J.-G. Park, J. Magn. Magn. Mater. **310**, 286 (2007).
- [90] T. Ekino, T. Takasaki, T. Suemitsu, T. Takabatake, H. Fujii, Physica **B312-313**, 221 (2002).
- [91] T. Kumigashira, T. Takahashi, S. Yoshii, and M. Kasaya, Phys. Rev. Lett. **87**, 67206 (2001).
- [92] H. Okumura, M. Matsunami, T. Nanba, T. Suemitsu, T. Yoshino, T. Takabatake, Y. Isikawa, H. Harima, Physica **B312-313**, 218 (2002).
- [93] M. Matsumura, T. Sasakawa, T. Takabatake, S. Tsuji, H. Tou, M. Sera, J. Phys. Soc. Jpn. **72**, 1030 (2003).
- [94] F. Ishii, Physica **B328**, 154 (2003).
- [95] D.T. Adroja, J.-G. Park, K.A. McEwen, K. Shigetoh, T. Sasakawa, T. Takabatake, and J.-Y. So, Physica **B378-380**, 788 (2006).
- [96] L. Havela, V. Sechovsky, P. Svoboda, H. Nakotte, K. Prokes, F.R. de Boer, A. Seret, J.M. Winand, J. Rebizant, J.C. Spirlet, A. Purwanto, and R.A. Robinson, J. Magn. Magn. Mater. **140-144**, 1367 (1995).
- [97] M. Diviš, M. Richter, and H. Eschrig, Solid State Commun. **90**, 99 (1994); M. Diviš, M. Olšovec, M. Richter, H. Eschrig, J. Magn. Magn. Mater. **104-107**, 1365 (1995); L. Havela, V. Sechovsky, P. Svoboda, M. Diviš, H. Nakotte, K. Prokeš, F. R. de Boer, A. Purwanto, R. A. Robinson, A. Seret, J. M. Winand, J. Rebizant, J. C. Spirlet, M. Richter, and H. Eschrig, J. Appl. Phys **76**, 6214 (1994); K. Prokeš, E. Brück, H. Nakotte, P. F. de Châtel, and F. R. de Boer, Physica **B 206&207**, 8 (1995).
- [98] S. Paschen, M. Baenitz, V.H. Tran, A. Rabis, F. Steglich, W. Carrillo-Cabrera, Yu. Grin, A.M. Strydom, P. de V. du Plessis, J. Phys. Chem. Solids **63**, 1183 (2002).
- [99] V.H. Trana, S. Paschen, A. Rabis, M. Baenitz, F. Steglich, P. de V. du Plessis, A.M. Strydom, Physica **B312-313**, 215 (2002).
- [100] S. Paschen, V.H. Tran, N. Senthilkumaran, M. Baenitz, F. Steglich, A.M. Strydom, P. de V. du Plessis, G. Motoyama, and N.K. Sato, Physica **B329-333**, 549 (2003).
- [101] S. Paschen, M. Baenitz, V. H. Tran, A. Rabis, F. Steglich, W. Carrillo-Cabrera, Y. Grin, A. M. Strydom, P. de V. du Plessis, J. Phys. Chem. Solids **63**, 1183 (2002).
- [102] V. H. Tran, S. Paschen, A. Rabis, N. Senthilkumaran, M. Baenitz, F. Steglich, P. de V. du Plessis, and A. M. Strydom, Phys. Rev. B **67**, 075111 (2003).
- [103] A. K. Rajarajan, A. Rabis, M. Baenitz, A. A. Gippius, E. N. Morozowa, J. A. Mydosh, and F. Steglich, Phys. Rev. **B76**, 024424 (2007).
- [104] G. Chełkowska, J.A. Morkowski, A. Szajek, J. Stępień-Damm, and R. Troć, Eur. Phys. J. **B35** 349 (2003)
- [105] R. Troć, J. Alloys Compd. **442**, **34** (2007).
- [106] P de V du Plessis, A M Strydom, R Troć, and L Menon, J. Phys.: Condens. Matter **13** 8375 (2001)
- [107] K.A. McEwen, D.T. Adroja, J.-G. Park, A.D. Hillier, R.I. Bewley, D. Fort, to be published (2008)
- [108] C. Gröber, and R. Eder, Phys. Rev. **B57**, R12659 (1998); B. Bucher, Z. Schlesinger, P. C. Canfield, Z. Fisk, Phys. Rev. Lett. **72**, 522 (1994).
- [109] W. Wang, X.P. Li, and D.H. Lee, Phys. Rev. **B47**, 11939 (1993); C. Sanchez-Castro, K. Bedell and B.R. Cooper, Phys. Rev. **B47**, 6879 (1993).
- [110] T. Kasuya *et al.*, J. Phys. (Paris), Colloq. **40**, C5-308 (1979).

---

\*Corresponding authors: d.t.adroja@rl.ac.uk